

# We are IntechOpen, the world's leading publisher of Open Access books Built by scientists, for scientists

6,900

Open access books available

185,000

International authors and editors

200M

Downloads

Our authors are among the

154

Countries delivered to

TOP 1%

most cited scientists

12.2%

Contributors from top 500 universities



WEB OF SCIENCE™

Selection of our books indexed in the Book Citation Index  
in Web of Science™ Core Collection (BKCI)

Interested in publishing with us?  
Contact [book.department@intechopen.com](mailto:book.department@intechopen.com)

Numbers displayed above are based on latest data collected.  
For more information visit [www.intechopen.com](http://www.intechopen.com)



## GaN Nanowires Fabricated by Magnetron Sputtering Deposition

Feng Shi

*College of Physics & Electronics, Shandong Normal University,  
P.R.China*

### 1. Introduction

GaN, as an attractive third-generation semiconductor material (III-V), has shown great prospect in applications of short wavelength blue and ultraviolet (UV) light-emitting devices (LEDs), microwave devices and high-power semiconductor devices, due to its unique physical properties such as wide band-gap (3.39 eV direct gap at room temperature), high thermal conductivity, high electron saturated mobility, high thermal stability, and so on (Fasol, 1996; Nakamura, 1998; Morkoc & Mohammad, 1995; Han et al., 1997).

As we all know, GaN have three kinds of structure: hexagonal wurtzite ( $\alpha$ -phase), cubic blende ( $\beta$ -phase) salt mine (NaCl-type compound square structure), which are shown as Figure 1.

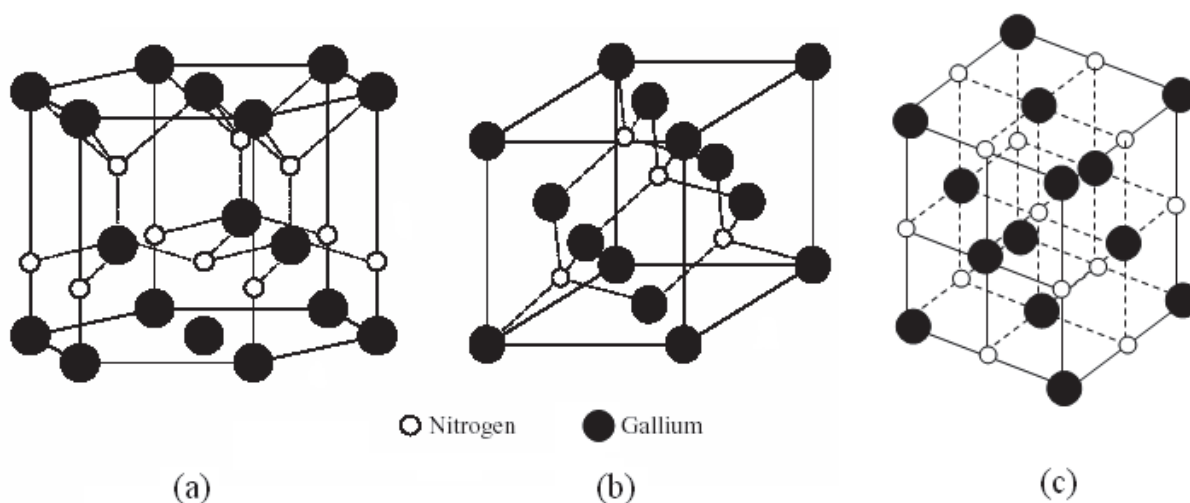


Fig. 1. The crystal structures of GaN. (a) Wurtzite Structure; (b) Blende Structure; (c) Salt Mine Structure.

In the past decades, a lot of man-powers, materials and financial resources have been put to study GaN by many countries, especially GaN nanostructures (nanowires, nanorods and nanobelts). One-dimensional GaN nanostructure has potential applications in the fields of full-color panel displays and nanometer electronic devices with high electron migration rate (Lauhon, 2002; Ham et al., 2006). However, the growth of GaN nanostructures with high

crystalline quality is the pre-condition for the fabrication of GaN-based components. Recently, several techniques have been developed to fabricate one-dimensional GaN structures such as carbon nanotube-confined reaction (Han,1997), template-based growth method (Xu et al., 2006), direction reaction of metal Ga with  $\text{NH}_3$  (He, 2000), ammoniating  $\text{Ga}_2\text{O}_3/\text{Al}_2\text{O}_3$  films (Xue et al., 2004) and sublimation method (Li et al., 2000).

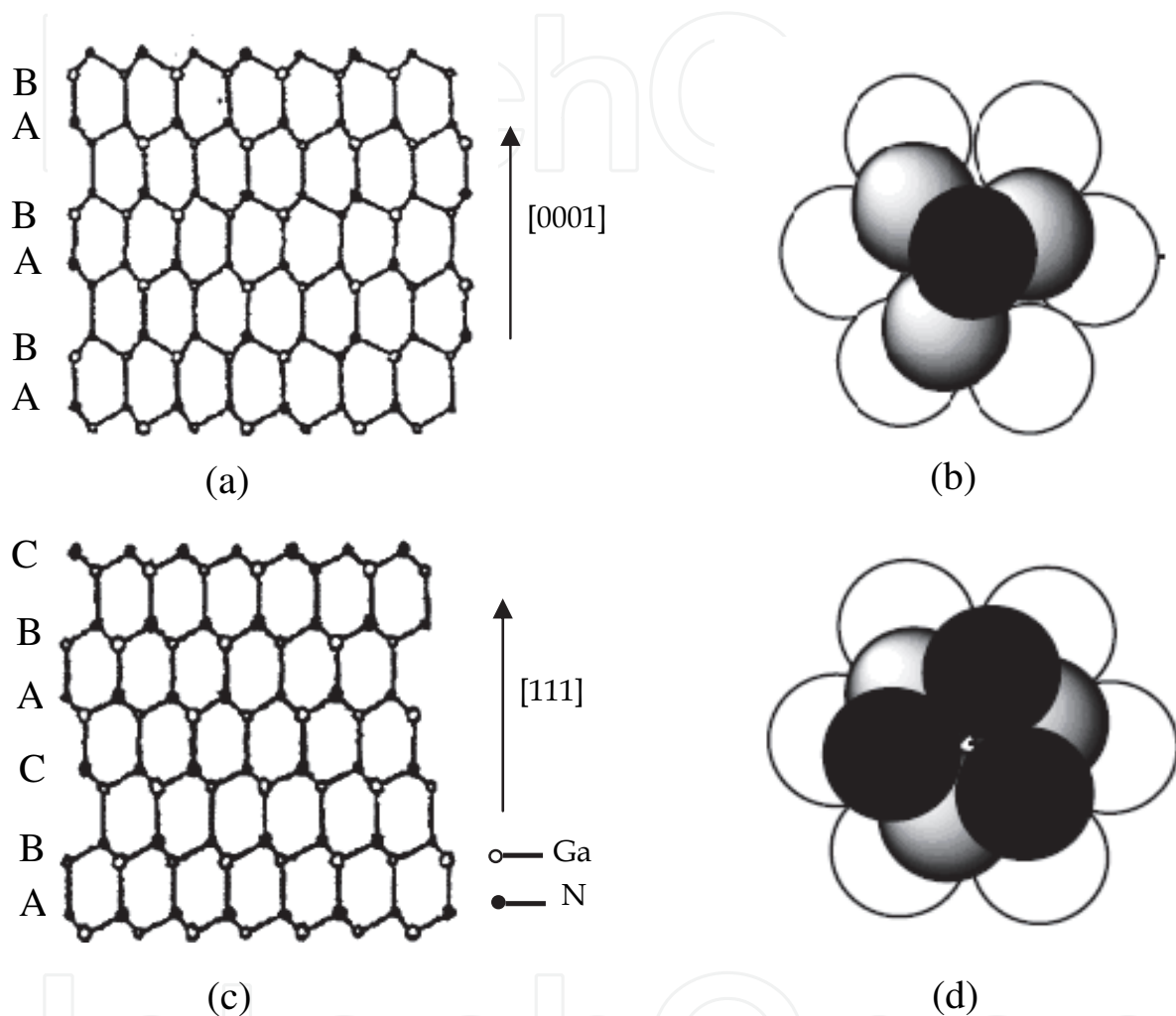


Fig. 2. Stacking Way of GaN: (a,b) Wurtzite Structure; (c,d) Blende Structure.

Of these methods, the metal catalyst-assisted growth is the most successful approach used popularly. According to our previous experimental results (Shi, 2010a, 2010b) the intermediate layer between Si substrates and  $\text{Ga}_2\text{O}_3$  had great influence on the modality and characteristics of the GaN nanostructures. Therefore, we attempted a novel route via Tb as the intermediate layer and synthesized unexpectedly large-scale GaN nanowires by ammoniation radio frequency (RF) magnetron sputtering method, *i.e.*, the transition metals of Ti, V, Cr, Co, Nb, Mo, Ta, and Tb (short for  $M_e$ ) are employed as catalyst materials forming the intermediate layer between Si substrate and  $\text{Ga}_2\text{O}_3$  film to grow unexpectedly large-scale GaN nanowires by ammoniation radio frequency (RF) magnetron sputtering method. That is, Ti, V, Cr, Co, Nb, Mo, Ta, and Tb ( $M_e$ ), the elements of transition metals, are employed as catalyst materials forming the intermediate layer between Si substrate and

Ga<sub>2</sub>O<sub>3</sub> films to growth one-dimensional GaN nanowires. In this chapter, high-quality GaN nanostructures, especially, nanowires, catalyzed by Ti, V, Cr, Co, Nb, Mo, Ta, and Tb have been fabricated on Si (111) substrate by ammoniating Ga<sub>2</sub>O<sub>3</sub> thin films. The fabrication condition, microstructure, morphology and photoluminescence (PL) optical properties were analyzed and the growth mechanism of GaN nanowires is further discussed. One-dimensional GaN nanowires are also fabricated by using MgO, TiO<sub>2</sub>, Al<sub>2</sub>O<sub>3</sub>, SiC, BN, and ZnO (short for C<sub>m</sub>) as intermediate layers. Through ammoniating Ga<sub>2</sub>O<sub>3</sub> films doped with Mg, high-quality P-typed GaN nanowires have been synthesized on Si(111) substrates. The growth mechanism of GaN nanowires are analyzed in detail.

The high-quality single GaN nanowires have also been fabricated by NiCl<sub>2</sub> Catalyzed Chemical vapor deposition and the growth mechanism of GaN nanowires are also analyzed in particular.

## 2. GaN nanowires fabricated by RF magnetron sputtering method

### 2.1 Catalyzed by transition metals of M<sub>e</sub>

#### 2.1.1 Experimental procedures

The growth method catalyzed by metallic M<sub>e</sub> is simple in fabrication progress and easy to control the size of the GaN nanostructures. Therefore, in our experiment, metallic M<sub>e</sub> and Ga<sub>2</sub>O<sub>3</sub> were deposited on the polished n-type Si(111) substrates in turn to form Ga<sub>2</sub>O<sub>3</sub>/M<sub>e</sub> films by sputtering the M<sub>e</sub> targets of 99.95 % purity and the sintered Ga<sub>2</sub>O<sub>3</sub> target of 99.99 % purity in a JCK-500A magnetron sputtering system. The sputtering time of M<sub>e</sub> and Ga<sub>2</sub>O<sub>3</sub> was 2 s ~ 5 s and 90 min with the thickness of 5 ~ 20 nm and 500 nm, respectively. The working conditions were, 150-Wand RF sputtering power of 13.56 MHz ; 20-Wand DC sputtering power; background pressure of 1.0×10<sup>-3</sup> Pa; and pure Ar (≥ 99.99%) as the working at a working pressure of 1~3 Pa. The distance between the target and the substrate was 8 cm. The sputtering progress was maintained at room temperature by the cooling system. After sputtering, the samples were ammoniated in a conventional tube furnace at atmosphere of pure NH<sub>3</sub> gas with purity of 99.999% under the temperatures of 800 °C ~ 1000 °C for 10~20 min. After being ammoniated, the samples were taken out for characterization.

The microstructure, composition, morphology and optical properties of the samples were studied using X-ray diffraction (XRD, Rigaku D/max-rB,Cu, K<sub>α</sub>, λ=1.54178 Å), FT-IR spectrophotometer with Mg X-ray source (FTIR, Bruker TENSOR27), X-ray photoelectron spectroscopy (XPS, Microlab MKII), scanning electron microscope (SEM, Hitachi S-570), high-resolution transmission electron microscope (HRTEM, Philips TECNAI-20), and photoluminescence spectroscopy (PL, LS50-fluorescence spectrophotometer).

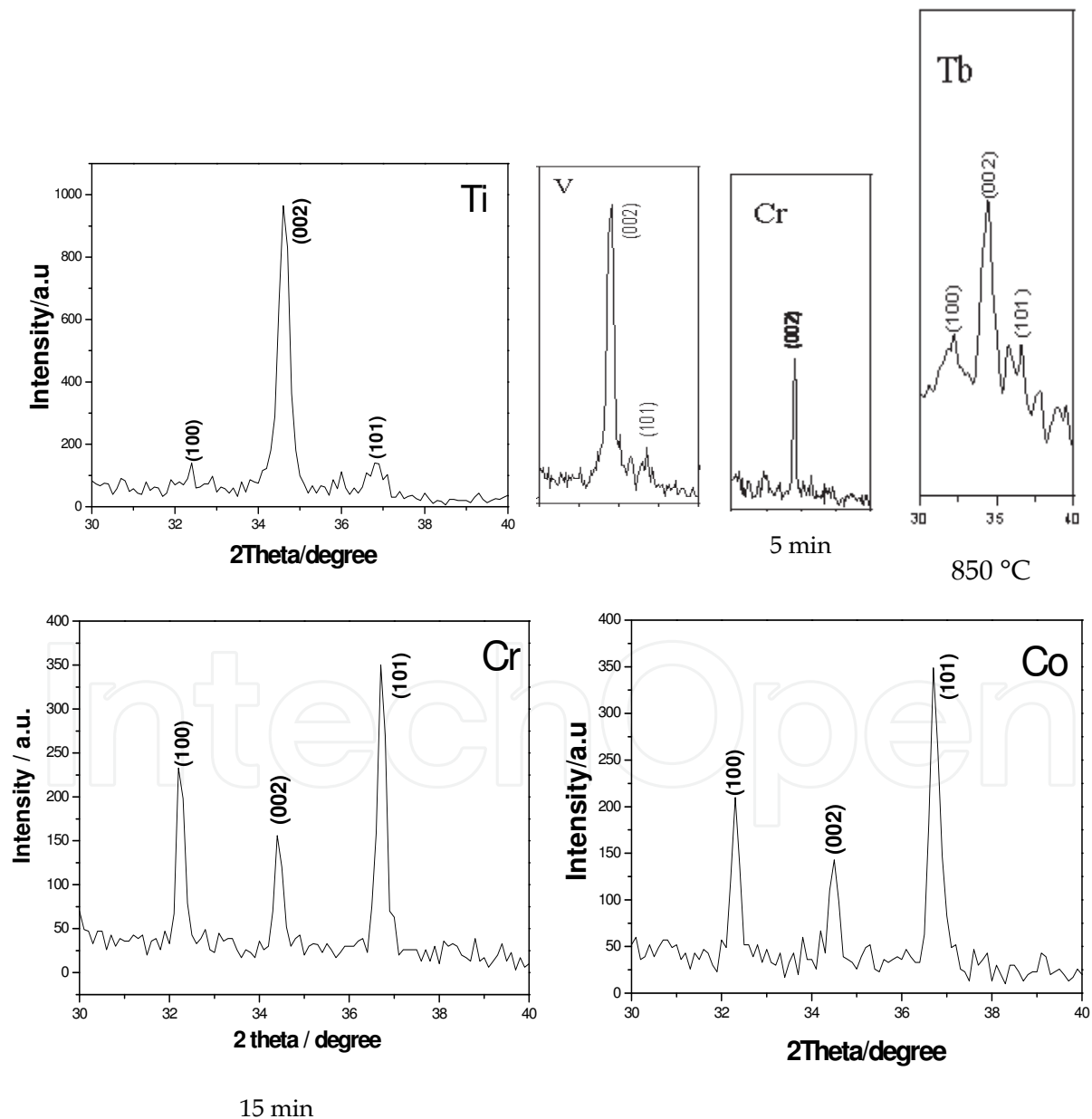
#### 2.1.2 Results and discussion

Figure 3 show the X-ray diffraction pattern of the samples grown at different temperatures with different transition metals.

As shown in Figure 3, the samples after ammoniation are hexagonal wurtzite GaN with lattice constant of  $a = 0.3186$  nm and  $c = 0.5178$  nm, and the diffraction peaks located at about  $2\theta = 32.3^\circ$ ,  $34.5^\circ$ , and  $36.7^\circ$  correspond to (100), (002) and (101) planes, which are consistent with the reported values for bulk GaN (Perlin, 1992). No peak of Ga<sub>2</sub>O<sub>3</sub>, M<sub>e</sub> or M<sub>e</sub>O is observed, indicating that neither Ga<sub>2</sub>O<sub>3</sub>, M<sub>e</sub> metal nor M<sub>e</sub>O coats the sample surface,

which indicates that these transitional elements take great catalytic action for the growth of GaN nanostructures.

Figure 3 tells us that at special conditions, the GaN nanostructures can grow along preferred (002) plane catalyzed by transitional elements of Ti, V, Cr, and rare-earth of Tb. While the GaN nanostructures can't grow along preferred plane by transitional elements of Nb, Mo, Co, and Ta. That is, the GaN nanostructures can grow along preferred (002) plane catalyzed by the first elements of the II, III, IV subgroups on the Periodic Table of chemical elements, except the other elements. This is a noticed phenomenon deserved further study. Ammoniating times and temperatures have great influence on the crystalline quality of the samples. The sample catalyzed by Cr can form preferred (002) plane ammoniated for 5 min, and the sample catalyzed by Tb can form preferred (002) plane ammoniated at 850 °C, which can be shown as Figure 4.



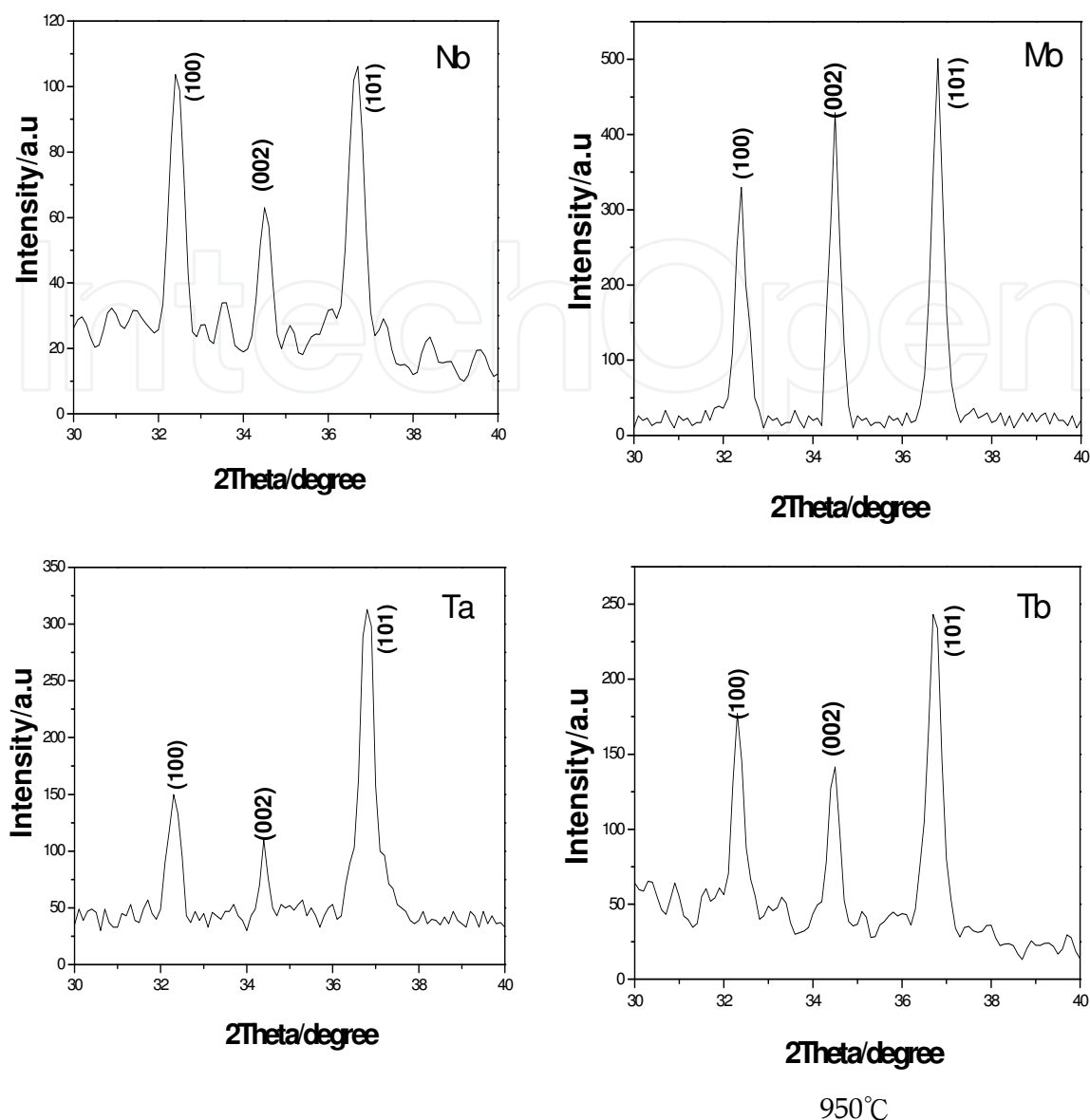


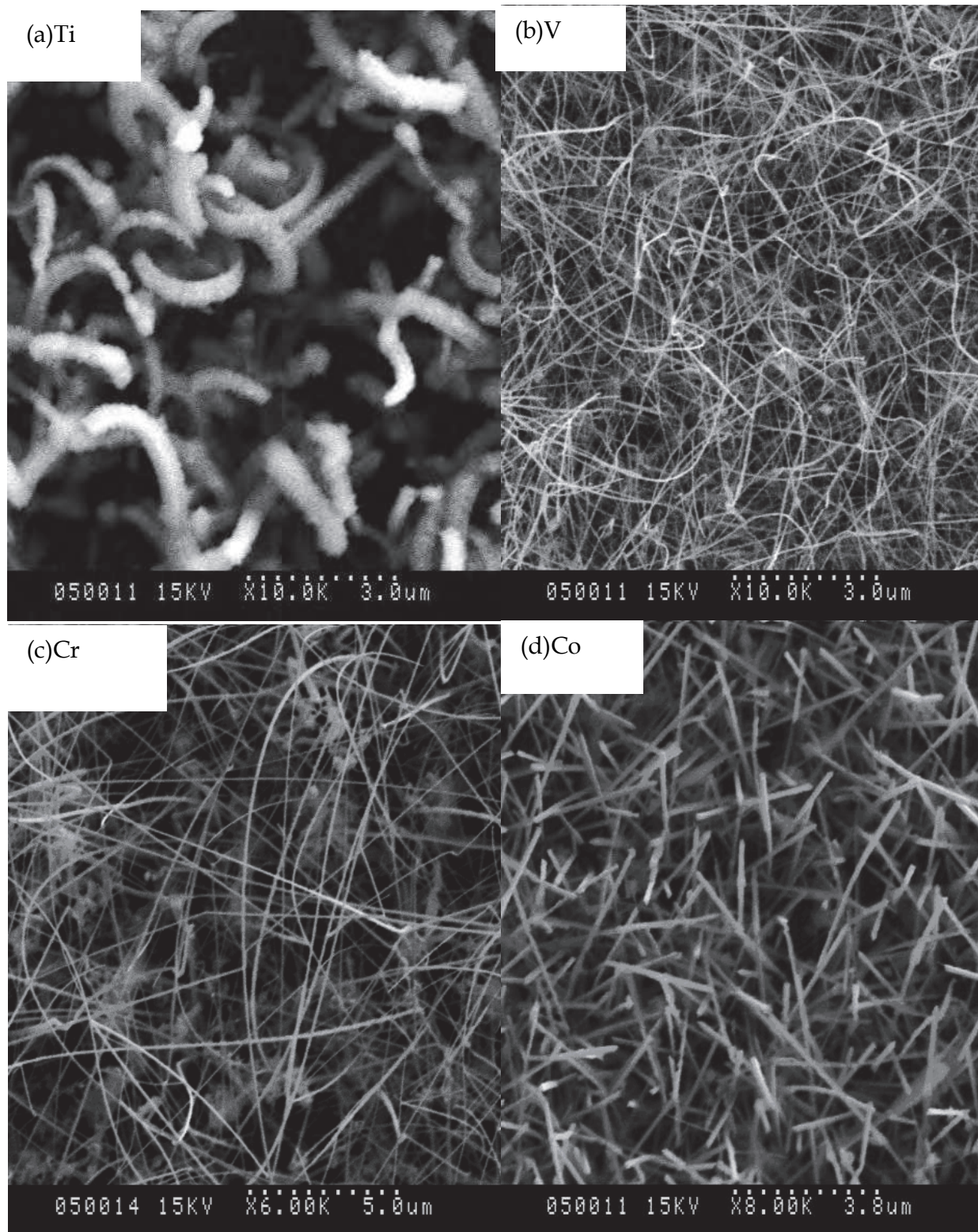
Fig. 3. X-ray diffraction pattern of the samples grown at different temperatures with different transition metals.

As shown from Figure 4, a large amount of one-dimensional nanowires distribute on the sample surfaces with high crystalline quality after catalyzed by V, Cr, Co, Nb, Mo, Ta, and Tb except catalyzed by Ti. Most of them are straight and smooth of uniform thickness along the spindle direction, and interlace with each other disorderly, having the size of about 50 ~100 nm in diameter and several tens of microns in length.

The diameters increase with the number of the protons, for example, the samples can form GaN nanowires when catalyzed by Ti, V, and Cr, however, with the increase in the protons, nanorods can be formed, such as the sample catalyzed by Co, as shown in Figure 4d. For Cr, and Co, the comparison is the most obvious.

As for V, Nb, and Ta, which are of the same sub-group, nanowires can be formed catalyzed by V, however, nanorods can be formed when catalyzed by Nb and Ta. Cr and Mo are of the same subgroup, the sample catalyzed by Cr can form nanowires, while after catalyzing by Mo, nanorods can be formed.

In short, the catalytic action increases with the increase in the number of the protons at the same line of the Periodic Table of chemical elements, and the morphology become obvious. And the same law exists in the same row.



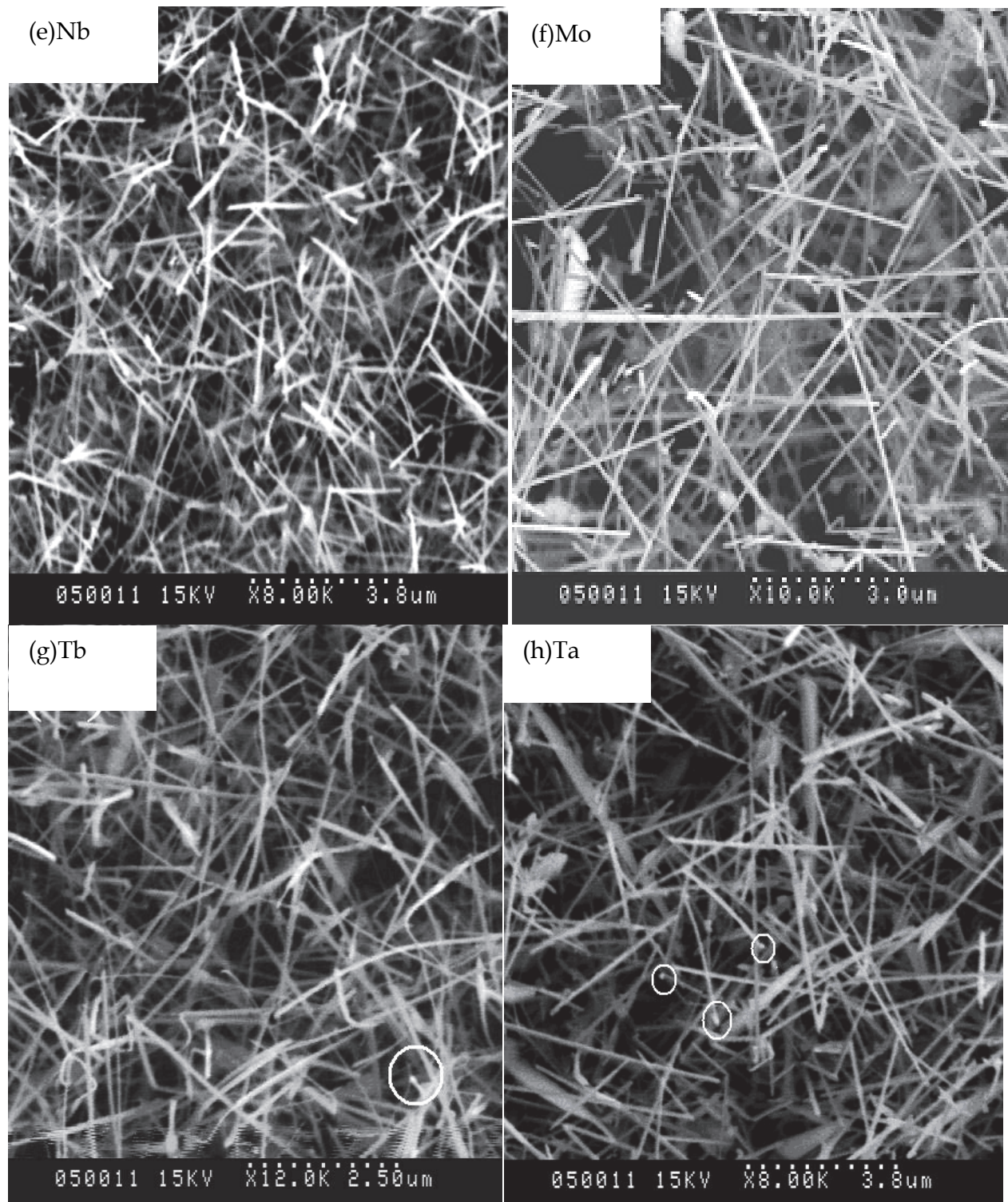


Fig. 4. SEM images of the samples catalyzed by different transition metals.

Ammoniating temperatures have great influence on the morphology of the sample catalyzed by Cr, which are shown in Figure 4c and Figure 5. In Figure 4c, nanowires are formed in the sample ammoniated at 950 °C, however, nanorods are formed ammoniated at 1000 °C, as shown in Figure 5.

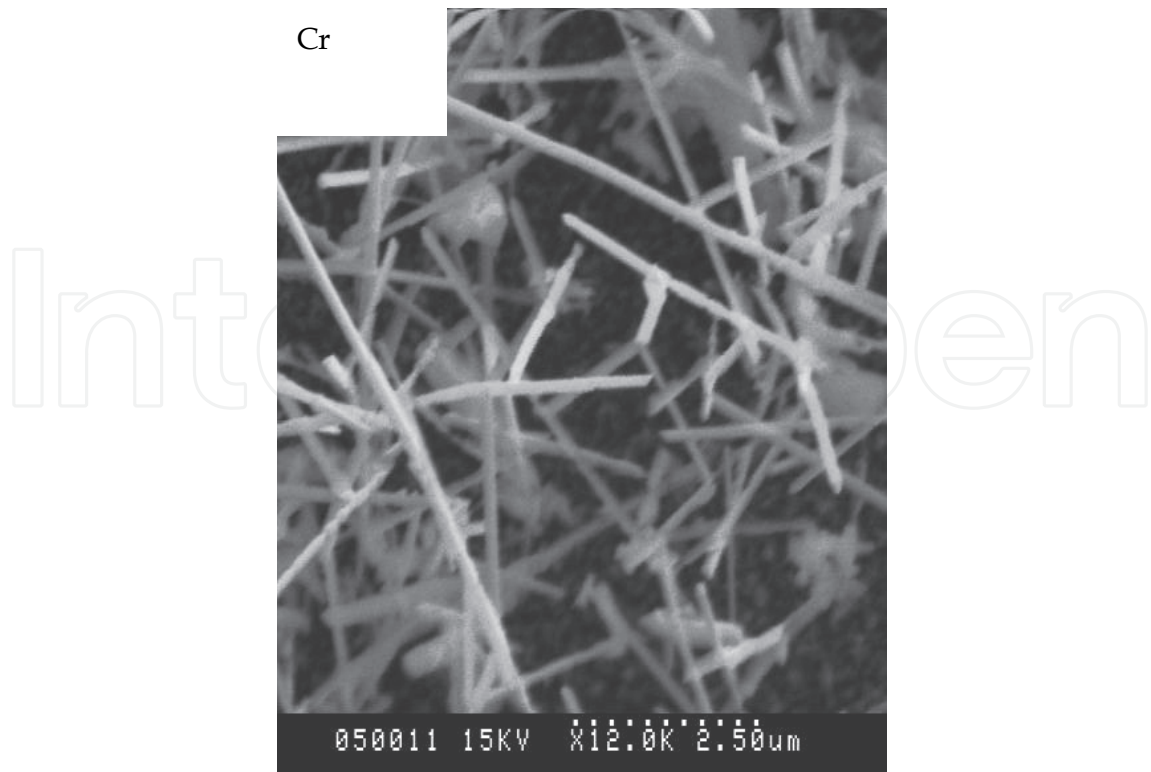


Fig. 5. SEM image of the sample grown at 1000 °C catalyzed by Cr.

Figure 6 show the TEM, selected area electron diffraction (SAED) and HRTEM images of an individual GaN nanowire. (a) TEM and SAED images,(b) HRTEM image.

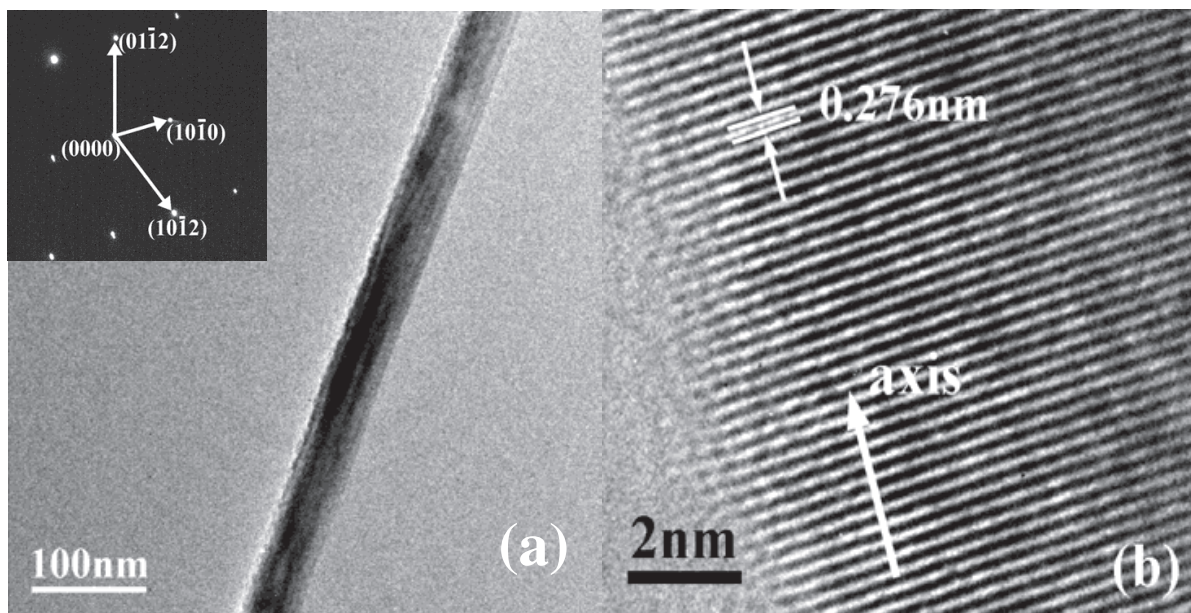


Fig. 6. TEM, selected area electron diffraction (SAED) and HRTEM images of an individual GaN nanowire. (a) TEM and SAED images,(b) HRTEM image.

As seen in Figure 6a, the nanowire is straight and smooth with uniform thickness in diameter and the diameter of nanowire is about 30 nm. Meanwhile, it shows the GaN nanowire is solid structure while not hollow tubular structure. Diffraction spots from

SAED are regular which shows GaN nanowire is monocrystal with hexagonal wurtzite structure. Seen from Figure 6b, HRTEM lattice image of straight GaN nanowire, the well-spaced lattice fringes in the image indicate a single crystal structure of GaN nanowires with high crystalline quality. The crystal plane spacing of nanowire is about 0.276 nm, which corresponds to (100) crystal plane spacing (0.276 nm) of hexagonal GaN single crystal.

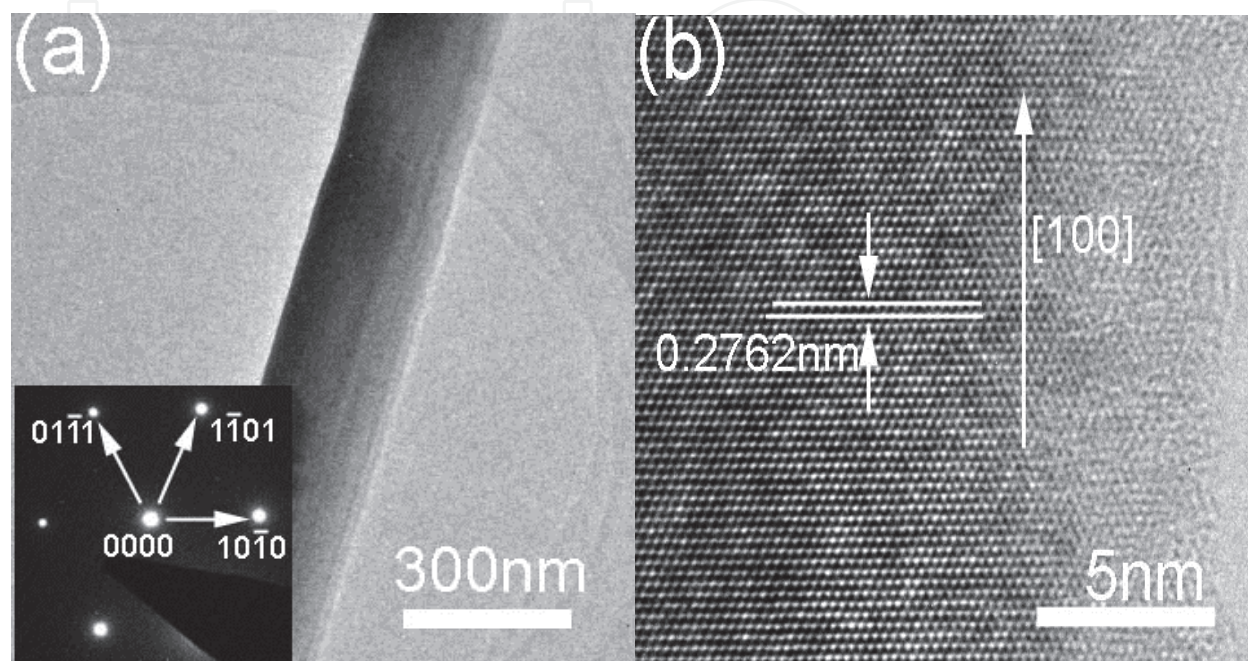


Fig. 7. TEM, selected area electron diffraction (SAED) and HRTEM images of an individual GaN nanorod. (a) TEM and SAED images, (b) HRTEM image.

Figure 7a shows that the nanorod is straight and smooth, of 150 nm in diameter. As seen from Figure 7b, HRTEM lattice image of the straight GaN nanorod, the well-spaced lattice fringe in the image indicates that the GaN nanorods have high crystalline quality with less dislocations and defects. The crystal plane spacing of the nanorod is about 0.2762 nm, which is less than that of (100) crystal plane spacing (0.276 nm) of hexagonal GaN single crystal (Monemar, 1974). The growth direction of this nanorod is parallel to [100] orientation. Diffraction spots from SAED (the inset in Figure 7a) are regular and corresponding to the diffraction direction of  $\bar{1}2\bar{1}3$ , which shows the GaN nanorod is monocrystal with hexagonal wurtzite structure.

We used different  $M_c$  elements to catalyze GaN samples and they were ammoniated at different temperatures and different times, nanowires and nanorods can be observed with clear surface, and we take the Mo as an example. Figure 8. FTIR patterns of the sample catalyzed by Mo after ammoniation at 950 °C for different times.

As seen in Figure 8, there are three well-defined prominent absorption bands, located at 564.07  $\text{cm}^{-1}$ , 608.94  $\text{cm}^{-1}$ , and 1102.31  $\text{cm}^{-1}$ . The band located at 564.07  $\text{cm}^{-1}$  corresponds to Ga-N stretching vibration ( $E_1(\text{TO})$  mode) in hexagonal type GaN crystal (Yang, 2002), and the other two bands are related to the Si substrate. The band located at 608.94  $\text{cm}^{-1}$  is associated with the local vibration of substituted carbon in the Si crystal lattice (Ai et al, 2007), whereas the band located at 1102.31  $\text{cm}^{-1}$  is attributed to the Si-O-Si asymmetric

stretching vibration because of the oxygenation of Si substrate (Sun,1998). There is no Ga-O bond and other absorption band in the spectrum (Demichelis, 1994), therefore, Ga<sub>2</sub>O<sub>3</sub> films react with NH<sub>3</sub> completely at 950 °C for 15 min and form hexagonal type GaN crystal, which is the same as the results of the XRD. The Ga-N bond intensity of the sample whose ammoniating time is 20 min is stronger than those of the other two samples, which proves the sample has the highest crystalline quality, and is also the same as the results of the XRD.

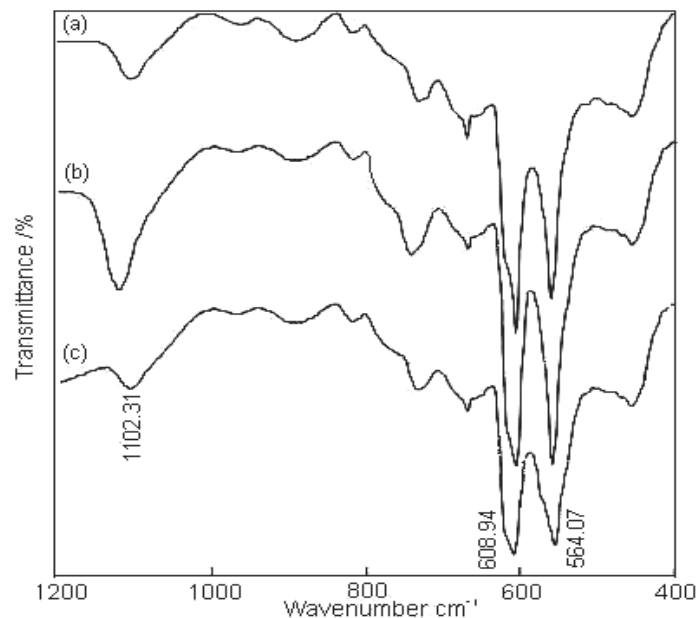


Fig. 8. FTIR patterns of the sample catalyzed by Mo after ammoniation at 950 °C for different times. (a) 15 min; (b) 20 min; (c) 25 min.

We have tested other samples which were ammoniated by other M<sub>e</sub> elements, the composition can be observed clearly by FTIR, and only GaN exists. In short, catalyzed by M<sub>e</sub>, the ammoniation reaction was complete and Ga<sub>2</sub>O<sub>3</sub> has turned to GaN completely.

Figure 9 shows the XPS images of N1s, Ga2p, Ga3d, and O1s for GaN synthesized at the ammoniating temperature of 950 °C, respectively.

Figure 9a shows the general scan in the binding energy ranging from 0 eV to 600 eV and the main components are Ga, C, N, and O with XPS peaks at the location of Ga2p<sub>3/2</sub> (1177.16 eV), Ga2p<sub>1/2</sub> (1144.10 eV), Ga3d (20.2 eV), N1s (396.1 eV) and O1s (530.3 eV).

The core level of Ga has a positive shift from elemental Ga, as shown in Figure 9b. This shift in the binding energies of Ga and N confirms the bonding between Ga and N and the absence of elemental gallium. As seen in Figure 9c, The binding energies of Ga2p<sub>3/2</sub> and Ga2p<sub>1/2</sub> are 1117.8 eV and 1144.5 eV, respectively, which are consistent with the results of Wei (Wei et al., 2005) whereas the banding energies of Ga element are 1116.6 eV (Elkashef et al., 1998) · 1118.5 eV (Kingsley et al., 1995) and 1119.2 eV (Sasaki et al.,1998). No bond formation is observed between Ga and O as the Ga3d spectrum does not show any satellite peak corresponding to β-Ga (Ishikawa et al., 1997) shows the Ga atom existing only as combined GaN, not Ga<sub>2</sub>O<sub>3</sub>. Quantification of the peaks shows that the atomic ratio of Ga to N is approximately 1:1.

As observed, the energy peak for N1s shown in Figure 9d is centered at 396.1eV, instead of 399 eV (binding energy of N element existing as atomic style), similar to the results of

Li (397.4 eV) (Li et al., 1997) and Veal (397.6 eV) (Veal et al., 2004), i.e., N atom exists as a nitride. The width and slight asymmetry of the N1s peak are attributed to N-H<sub>2</sub> and N-H<sub>3</sub> formation due to the interaction between N<sub>2</sub> and NH<sub>3</sub> at the GaN film surface (King,1999).

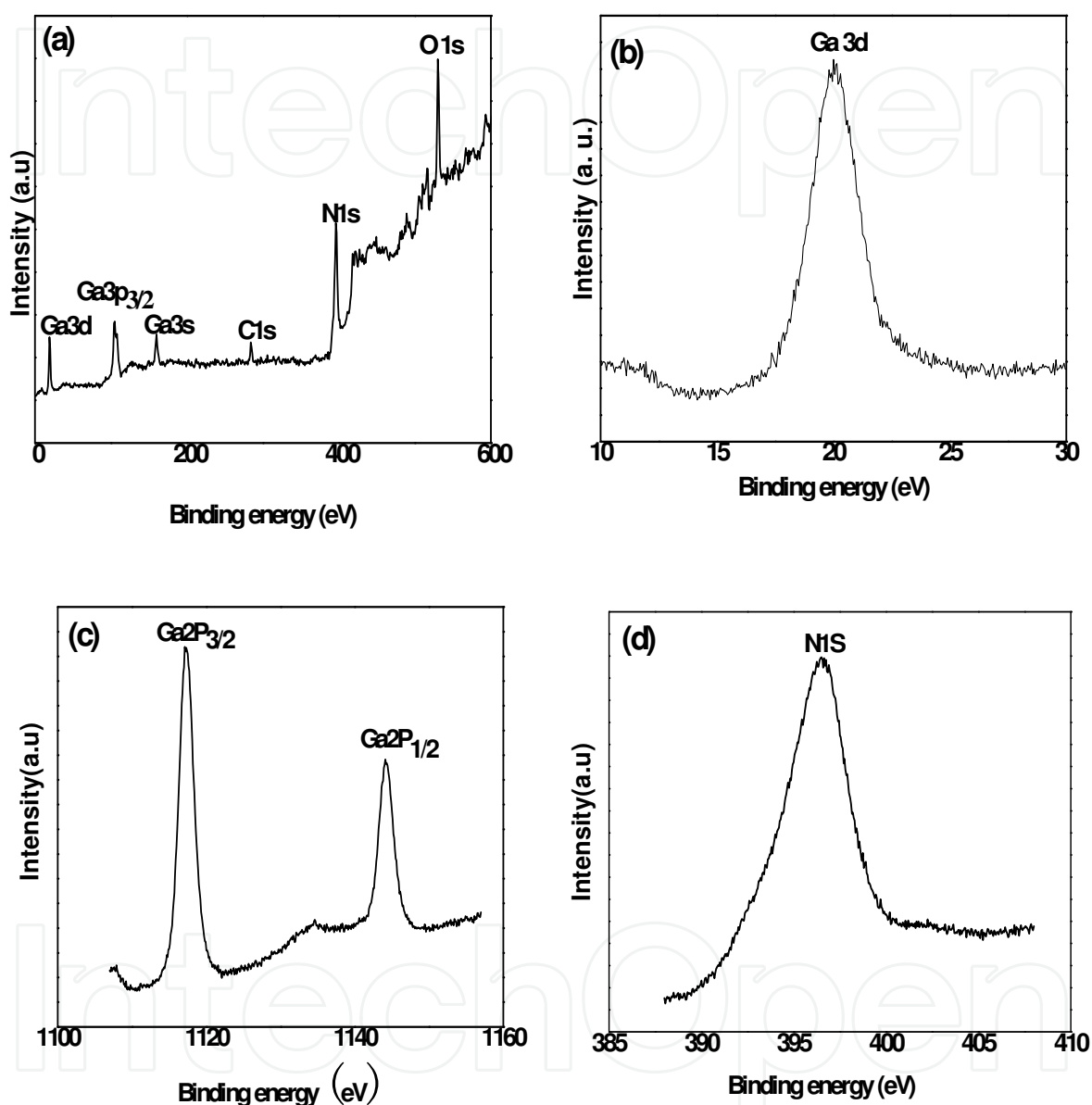


Fig. 9. XPS spectra of the sample after ammoniation at 950 °C for 15 min (Cr). (a) general scan spectrum;(b) Ga3d band; (c) Ga2p<sub>1/2</sub> and Ga2p<sub>3/2</sub> bands; (d) N1s band.

The elements of C and O arise from the surface pollution of the sample (Monemar,1974) . The O1s peak centered at 530.7 eV. According to Amanullah et al (Amanullah et al., 1998), generally, the O1s peak had been observed in the binding energy region of 529-535 eV, and the peak around 529-530 eV is ascribed to lattice oxygen. For chemisorbed O<sub>2</sub> on the surface the binding energy ranged from 530.0 eV to 530.9 eV. Therefore, the O1s peak in the present work is part of chemisorbed oxygen.

In short, XPS analysis shows that  $\text{Ga}_2\text{O}_3$  reacts with  $\text{NH}_3$  completely and forms GaN after ammoniation at  $950^\circ\text{C}$  for 15 min, similar to the results of the XRD and FTIR analysis.

Figure 10 is the photoluminescence spectrum of the samples grown at different temperatures for 15 min (Tb).

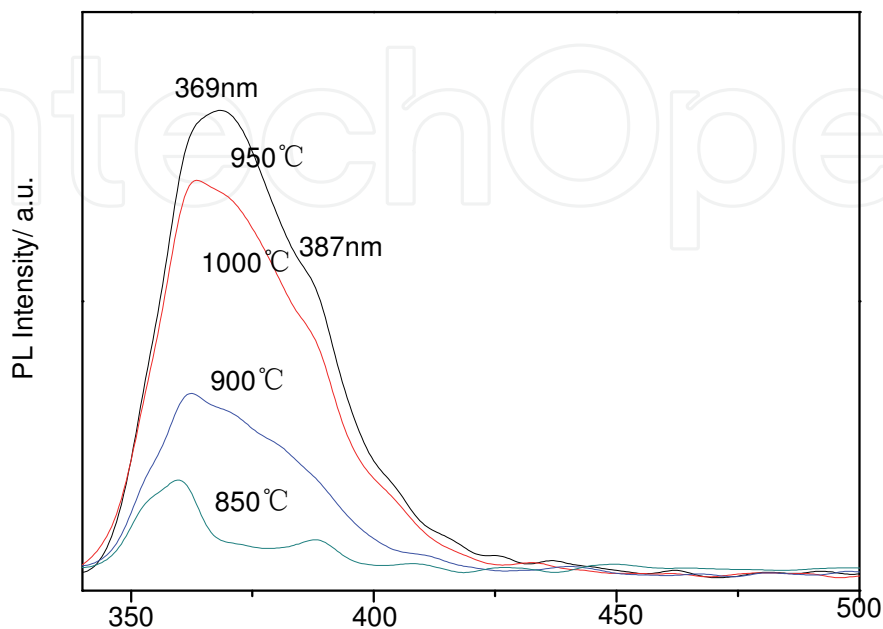


Fig. 10. Photoluminescence spectrum of the samples grown at different temperatures for 15 min (Tb). (a)  $850^\circ\text{C}$ , (b)  $1000^\circ\text{C}$ , (c)  $900^\circ\text{C}$ , (d)  $950^\circ\text{C}$ .

Figure 10 shows there is a strong UV emission peak centered at 369 nm corresponding to near band-edge emission of hexagonal GaN (Xiao et al., 2005). Because the diameter of the nanorod is much larger than the Bohr exciton radius (11 nm), beyond the work scope of quantum confinement effects, no blue-shift is discerned when compared with bulk GaN, but a small red-shift has occurred when compared with 365 nm reported by reference (Monemar, 1974). The reason of red-shift is probably related with band gap change caused by the tensile stress of one-dimensional GaN nanomaterials along the axial direction (Bae et al., 2003). The corresponding binding energy (eV) is 3.36 eV and thus it is smaller than binding energy of bulk GaN with 3.39 eV. Meanwhile, a weak light emission band centered at 387 nm can be observed, too, which is due to the excitons bound to surface or other structure defects (Schlager, 2006). The luminescence properties have been affected by more probabilities of defects and surface states due to larger surface area, comparing with the GaN epitaxial layer. The locations of the two emission peaks do not change but the intensity of the emission peaks changes obviously with the variation of the ammoniating temperature, which indicates the optical properties are closely related with the ammoniating temperature. The luminous intensity of GaN nanostructures is at its highest at  $950^\circ\text{C}$ .

Figure 11 shows the photoluminescence spectra of the samples (Cr) nitridized at  $950^\circ\text{C}$  for different nitridation times.

Figure 11 shows there is only one strong ultraviolet emission peak centered at 362 nm, which is close to the result of 365 nm reported by reference (Monemar, 1974). A blue-shift

occurs, which is attribute to quantum confinement effect (Chen et al., 2001; Liu et al., 2001). The site of the strong emission peak does not change but the intensities of the emission peak changes obviously with the viriation of nitridation time. The intensity of the emission peak reaches its best after nitridation for 15 mins, which shows that the optical properties of GaN nanowire structures significantly depend on ammoniating times.

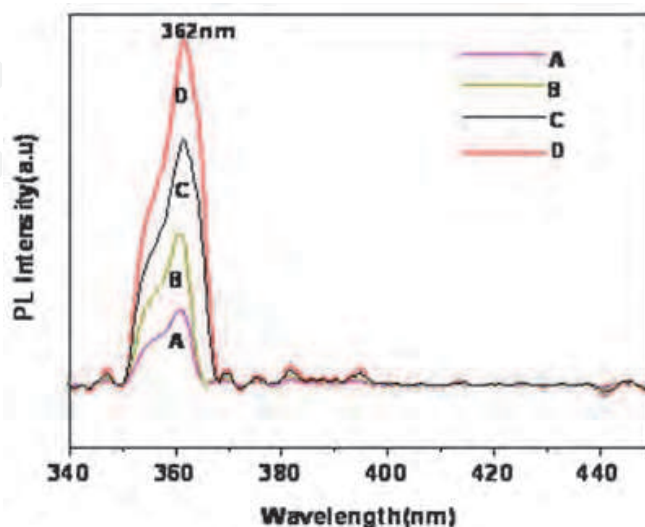


Fig. 11. The photoluminescence spectra of the samples (Cr) nitridized at 950 °C for different nitridation times of (a) 20 mins; (b) 5 mins; (c) 10 mins; (d) 15 mins.

Different metallics have great influence on the optical properties of GaN nanowires. We summarized the data after testing all the samples catalyzed by Ti, V, Cr, Co, Nb, Mo, and Ta, which are listed in Table 1.

Ti 364nm	V 368.2nm	Cr 362nm	Co 370nm
	Nb 367.5nm	Mo 370.5nm	
	Ta 364nm		

Table 1. Wavelengths of strong UV emission peaks for the samples catalyzed by different  $M_e$ .

Table 1 shows that with the increase in the number of protons, the wavelength of the samples catalyzed by different elements can change their sites, i.e., blue-shift, red-shift, and then blue-shift, red-shift. In short, wavelength shifts to long wave, i.e., red-shift, with the increase in the number of the protons at the same line of the Periodic Table of chemical elements. While as for the same subgroup elements, from V to Nb to Ta, wavelength decreases, i.e, blue-shift.

Note: Cr is an exception, and the reason is unknown.

### 2.1.3 Growth mechanism

There are several growth mechanisms for one-dimension nanowires, One is vapor-liquid-solid (VLS) process (Sun et al., 2002), in which nanoparticles as catalysts are formed on the tip of nanowires. The other is VS mechanism (Wang et al., 2004), in which nanowires are

fabricated from the vapor of precursor directly, without a liquid state. For the GaN nanowires synthesized in our cases, VLS mechanism is dominant but not enough to explain the growth of the GaN nanowires.

The growth of one-dimensional nanowires are closely related to the defect energies because there are more broken bonds at defect sites with lower chemical potential and nanowires can grow from these defects. Less nanowires can form when GaN films were deposited on the single crystal Si substrate by MBE or MOCVD because there are less defects on the Si substrate surface and the surface energies are too low to provide enough energy for the growth of one-dimensional nanowires. One-dimensional nanowires can form after the intermediate layer is deposited on the Si substrate. The defects originating from the intermediate layer can change the energy distribution on the substrate surface and provide more energies for the growth of nanowires.

Figure 12 show the typical images of GaN nanostructures.

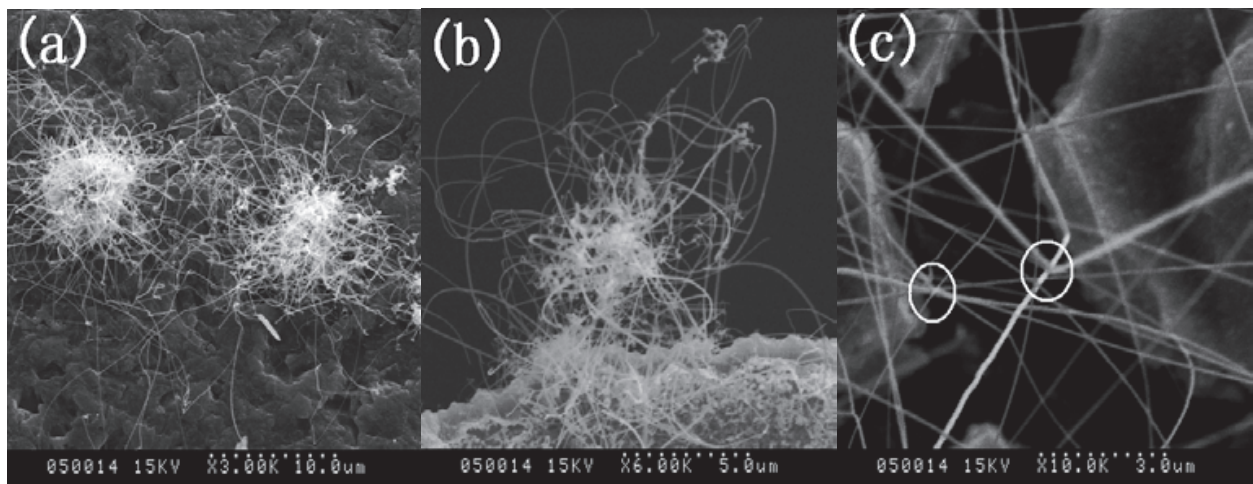


Fig. 12. (a) Cluster growth of one-dimensional GaN nanostructure; (b) Magnification of local area in image (a); (c) SEM image of single nanowire with nanoparticle on the tip.

During our experiments, we found that these nanowires grew as clusters-like structure, as shown in Figure 12a and Figure 12b, and distributed on the substrate surface scarcely. In Figure 12, there exist cluster-like nanowires and nanowires grow radially outward from the central nuclei. As identified in Figure 12c and Figure 4g, and 4h, there are nanoparticles on the tips of nanowires, which is the most noteworthy feature of the vapor-liquid-solid (VLS) mechanism. Therefore, we infer that metallic  $M_e$  forms the central nuclei during ammonation on the substrate surface and GaN nanowires occur from these nanoparticles. That is,  $M_e$  intermediate layers provide nucleation points for the formation of GaN crystalline nuclei and play an important role for the formation of GaN nanowires.

The growth procedure of nanowires is inferred and clarified as follows. Cr nanoparticles form and distribute on the substrate surface at ammonation temperature (Ohno et al., 2005) and thus many defects occur on the single crystal Si substrate surface, which has less defects originally. These defects energies have changed the energy distribution on the substrate surface. The broken bonds on the defect sites absorb dissociative gaseous state Ga and N atoms and form Cr-Ga-N structures continuously (as shown in Figure 13). We name this explanation as "defect energies confinement theory" (Shi et al., 2010c).

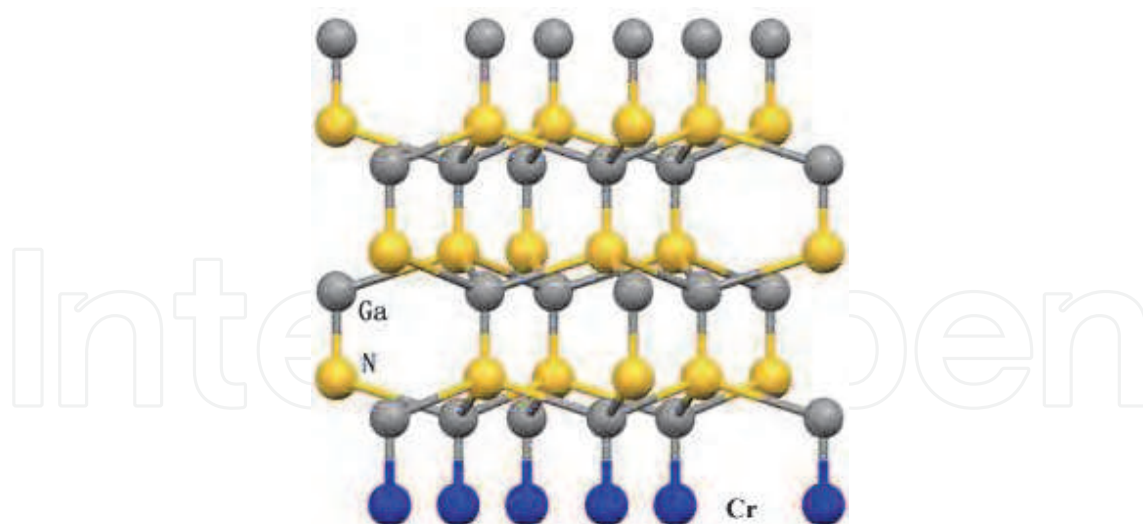
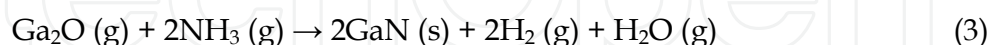
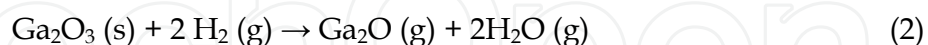


Fig. 13. Cr-Ga-N structures during the formation of GaN nanowires.

On the other hand,  $\text{NH}_3$  decomposes to  $\text{NH}_2$ ,  $\text{NH}$ ,  $\text{H}_2$  and  $\text{N}$  gradually when temperature reaches  $850^\circ\text{C}$  (Tang et al., 2000; Xue et al., 2005)  $\text{Ga}_2\text{O}_3$  particles are deoxidized to gaseous  $\text{Ga}_2\text{O}$  by  $\text{H}_2$  and next GaN molecules are synthesized through the reaction of  $\text{Ga}_2\text{O}$  and ammonia. GaN molecules occur by the reaction of gaseous  $\text{Ga}_2\text{O}$  and  $\text{NH}_3$  gases diffuse and move to the substrates, forming GaN crystalline nuclei. When GaN molecules carried by gas flow meet GaN crystallite nuclei, they can combine together immediately, therefore, GaN crystallite nuclei grow up gradually and single-crystal nanowires come into being. During the whole process, there are broken bonds on the nanowires surface and thus defect energies accumulate and absorb Ga- and N atoms from the surrounding saturated gas. When the concentration of gas reduces or when the defect energies of the nanowires fall to an insufficient level and can't absorb GaN nanowires, the growth of nanowires ends. From a macro perspective, the GaN nanowires formation on the substrate surface includes absorption, migration, nucleus formation, converging to islands, growth and desorption before they are formed into GaN nanowires.

The reaction formula are as follows:



We deposited  $\text{Ga}_2\text{O}_3$  on the silicon substrate without Cr intermediate layer under the same conditions but no nanowires were generated. Therefore, Cr is thought to be a nucleation point of the GaN nanowires and plays an important role as catalyst. The process of growth follows the vapor-liquid-solid (VLS) mechanism.

In short, both VLS and defects energy theory can explain the formation of the GaN nanowires.

#### 2.1.4 Summary

Large-scale GaN nanowires can be formed and the predominant phase of samples fabricated by magnetron sputtering method catalyzed by metallics of  $\text{M}_e$  is the hexagonal wurtzite

GaN crystal identified by XRD analysis; the existence of the Ga-N bond is established by the FTIR spectrum and N atom exists as nitride by XPS.

The GaN nanowires are single crystal with straight, smooth surface and uniform thickness along spindle direction, have the size of 30-80 nm in diameter and several tens of microns in length with high-quality crystalline.

At special conditions, the GaN nanostructures can grow along preferred (002) plane catalyzed by transitional elements of Ti, V, Cr, and rare-earth of Tb. While the GaN nanostructures can't grow along preferred plane by transitional elements of Nb, Mo, Co, and Ta. That is, the GaN nanostructures can grow along preferred (002) plane catalyzed by the first elements of the II, III, IV subgroups on the Periodic Table of chemical elements, except the other elements. This is a noticed phenomenon deserved further study.

Ammoniating times and temperatures have great influence on the crystalline quality of the samples. The sample catalyzed by Cr can form preferred (002) plane ammoniated for 5 min, and the sample catalyzed by Tb can form preferred (002) plane ammoniated at 850 °C.

The diameters increase with the number of the protons, for example, the samples can form GaN nanowires when catalyzed by Ti, V, and Cr, however, with the increase in the protons, nanorods can be formed, such as the sample catalyzed by Co. As for V, Nb, and Ta, which are of the same sub-group, nanowires can be formed catalyzed by V, however, nanorods can be formed when catalyzed by Nb and Ta. Cr and Mo are of the same subgroup, the sample catalyzed by Cr can form nanowires, while after catalyzing by Mo, nanorods can be formed. That is, the catalytic action increases with the increase in the number of the protons at the same line of the Periodic Table of chemical elements, with the morphology becoming obvious. And the same law exists in the same row.

Ammoniating temperatures have great influence on the morphology of the sample catalyzed by Cr, nanowires are formed in the sample ammoniated at 950 °C, however, nanorods are formed ammoniated at 1000 °C.

GaN nanowires have good optical properties, which can be tested by PL spectra. The optical properties of GaN nanowires greatly depend on the ammoniating temperatures and times. With the increase in the number of protons, the wavelength of the samples catalyzed by different elements can change their sites, i.e., blue-shift, red-shift, and then blue-shift, red-shift. In short, wavelength shifts to long wave, i.e., red-shift, with the increase in the number of the protons at the same line of the Periodic Table of chemical elements. While as for the same subgroup elements, from V to Nb to Ta, wavelength decreases, i.e., blue-shift. However, Cr is an exception, and the reason is unknown.

The growth procedure follows the VLS mechanism, and  $M_e$  acts as the nucleation point for GaN crystalline nuclei and plays an important role as catalyst during ammoniation process. Defect energies confinement theory can also be applied to explain the formation of GaN nanostructures.

## **2.2 GaN Nanowires catalyzed by intermediate layer of $C_m$**

### **2.2.1 Experimental procedures**

The experimental procedure is the same as the second section, i.e., GaN Nanowires Catalyzed by Transition Metallic of  $M_e$ , and the only difference between them lies in that the  $C_m$  and  $Ga_2O_3$  films were sputtered on Si (111) substrates by RF magnetron sputtering method, with the  $C_m$  (MgO,  $TiO_2$ ,  $Al_2O_3$ , SiC, BN, and ZnO) target of 99.99% purity and the sintered  $Ga_2O_3$  target of 99.999% purity. The thicknesses of the intermediate layers are of 10 nm ~ 200 nm.

The other conditions are the same as that stated in the second section of "GaN Nanowires Catalyzed by Transition Metallic of  $M_e$ ".

### 2.2.2 Results and discussion

Figure 14 show the X-ray diffraction patterns of the samples grown at different temperatures with different intermediate layer of  $C_m$ .

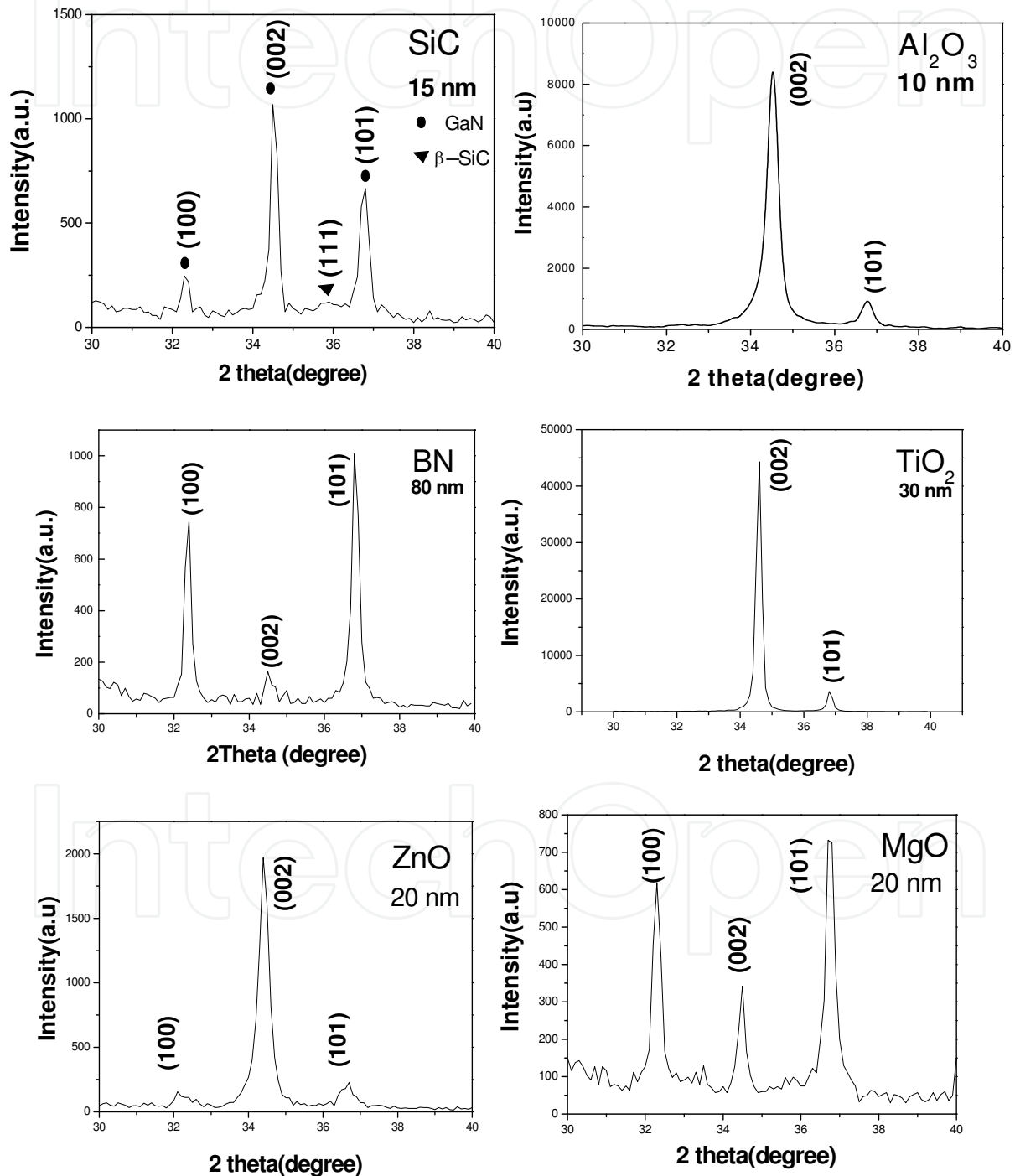
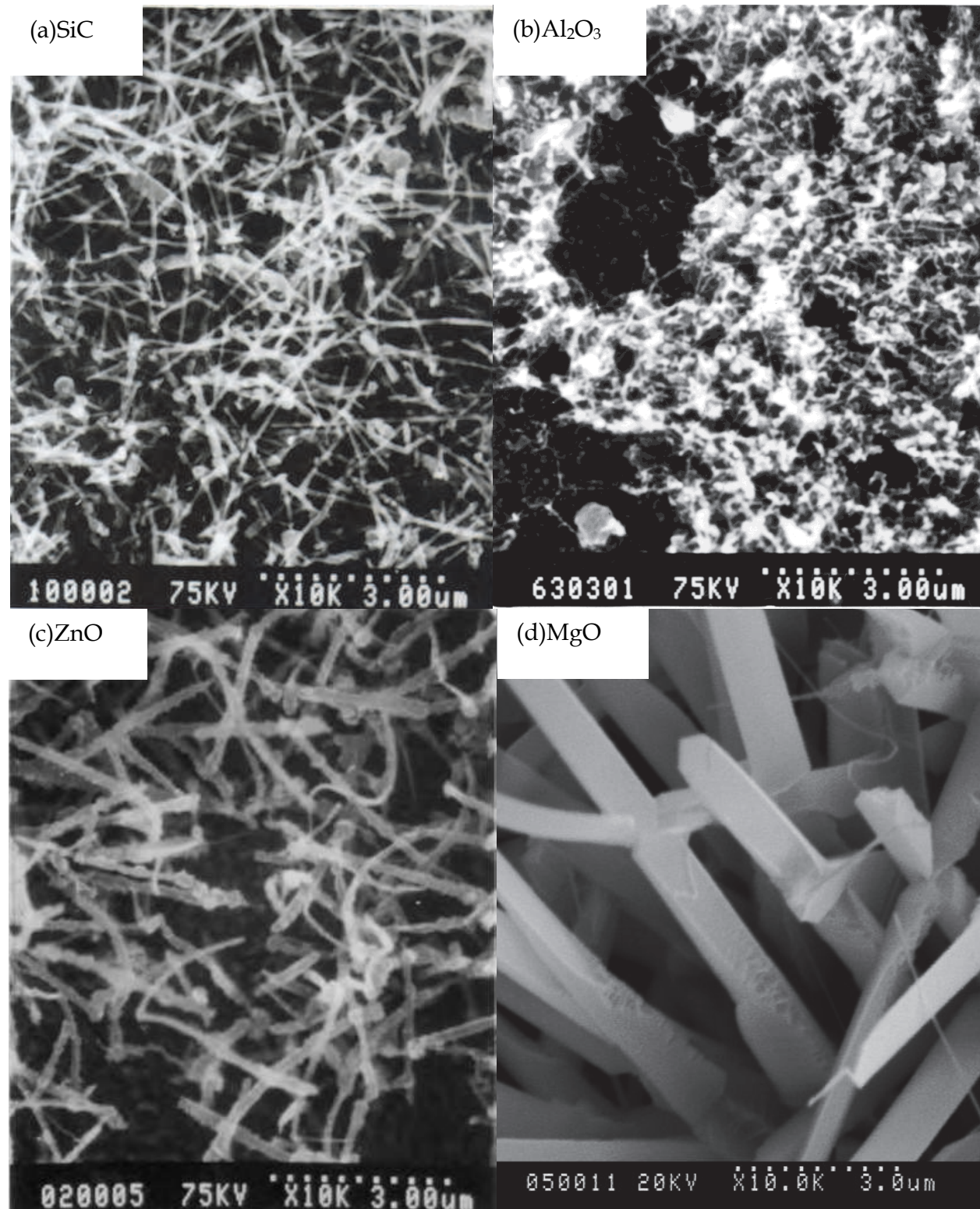


Fig. 14. X-ray diffraction pattern of the samples grown at different temperatures with different intermediate layer of  $C_m$ .

Figure 14 shows that GaN can grow along preferred (002) planes catalyzed by  $\text{Al}_2\text{O}_3$  (10 nm), ZnO (20 nm), and  $\text{TiO}_2$  (30 nm), which were fabricated at the optimal conditions. However, other samples can't grow along preferred (002) planes.

Figure 15 show the SEM images of the samples catalyzed by different intermediate layers of  $\text{C}_m$ .



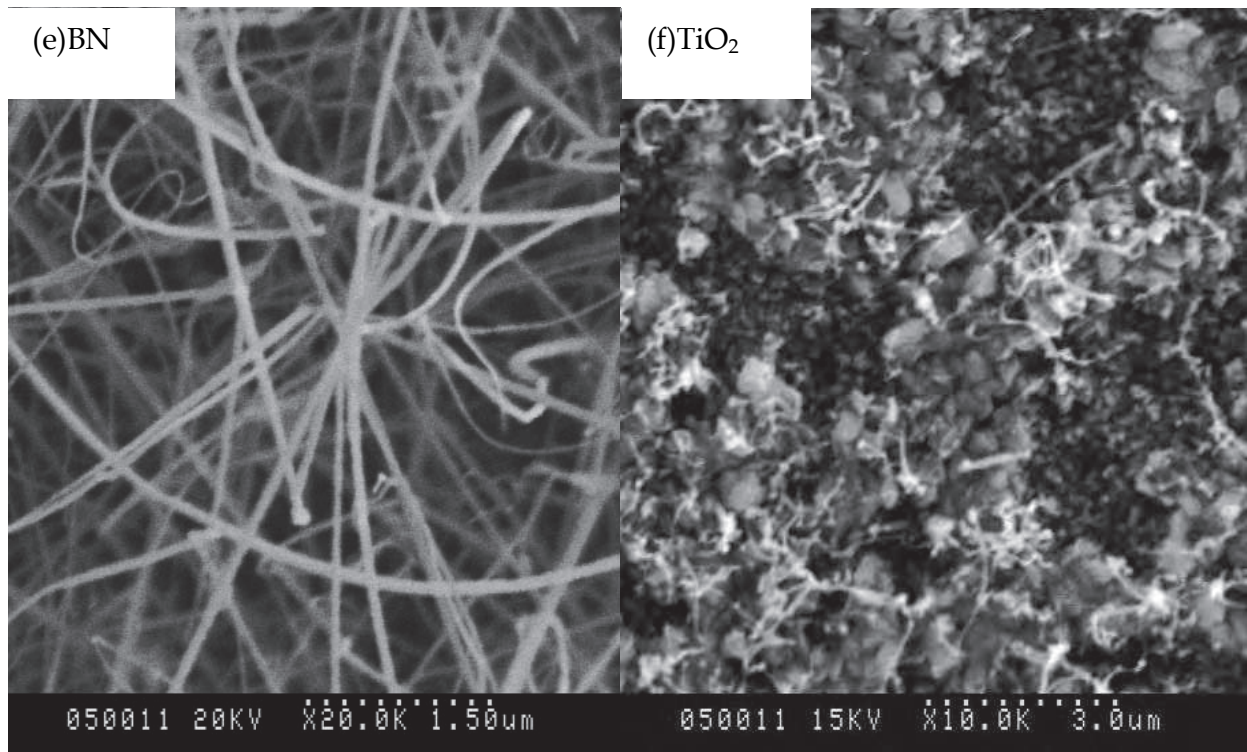


Fig. 15. SEM images of the samples catalyzed by different intermediate layers of C<sub>m</sub>.

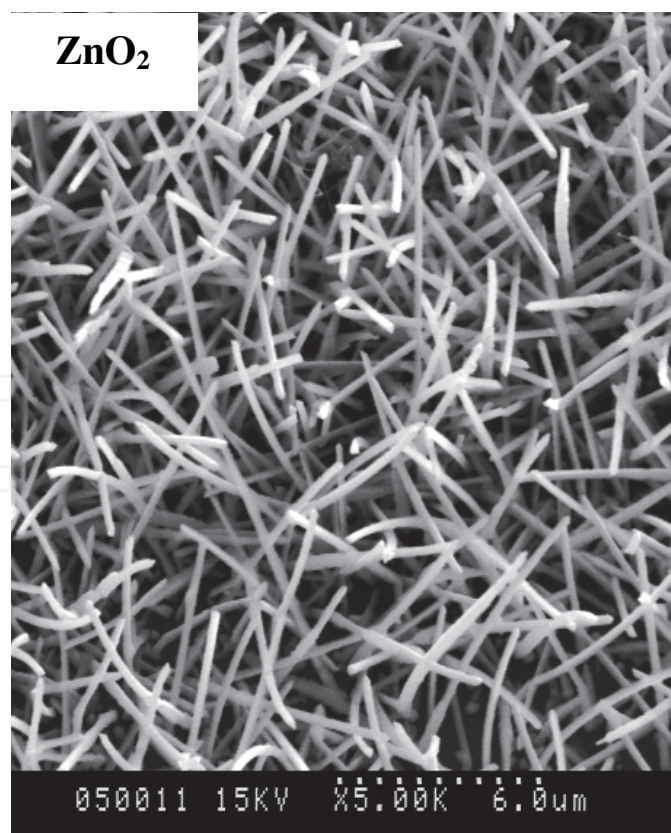


Fig. 16. SEM image of the sample catalyzed by 200 nm ZnO thin film as intermediate layer.

Figure 15 show that pure and clear GaN nanostructures can be formed with ZnO, MgO, and BN as intermediate layers. While as for the samples using SiC, Al<sub>2</sub>O<sub>3</sub>, and TiO<sub>2</sub> as intermediate layers, GaN nanostructures are vague. GaN nanowires are formed with ZnO, and BN as intermediate layers, and nanobelts are formed with MgO, as intermediate layers. When the thickness of ZnO increases form 20 nm to 200 nm, the sample can turn from GaN nanowires to nanorods, which is shown as Figure 16.

Figure 17. SEM images of the sample catalyzed by 20 nm MgO thin film as intermediate layer and ammoniated at different temperatures.

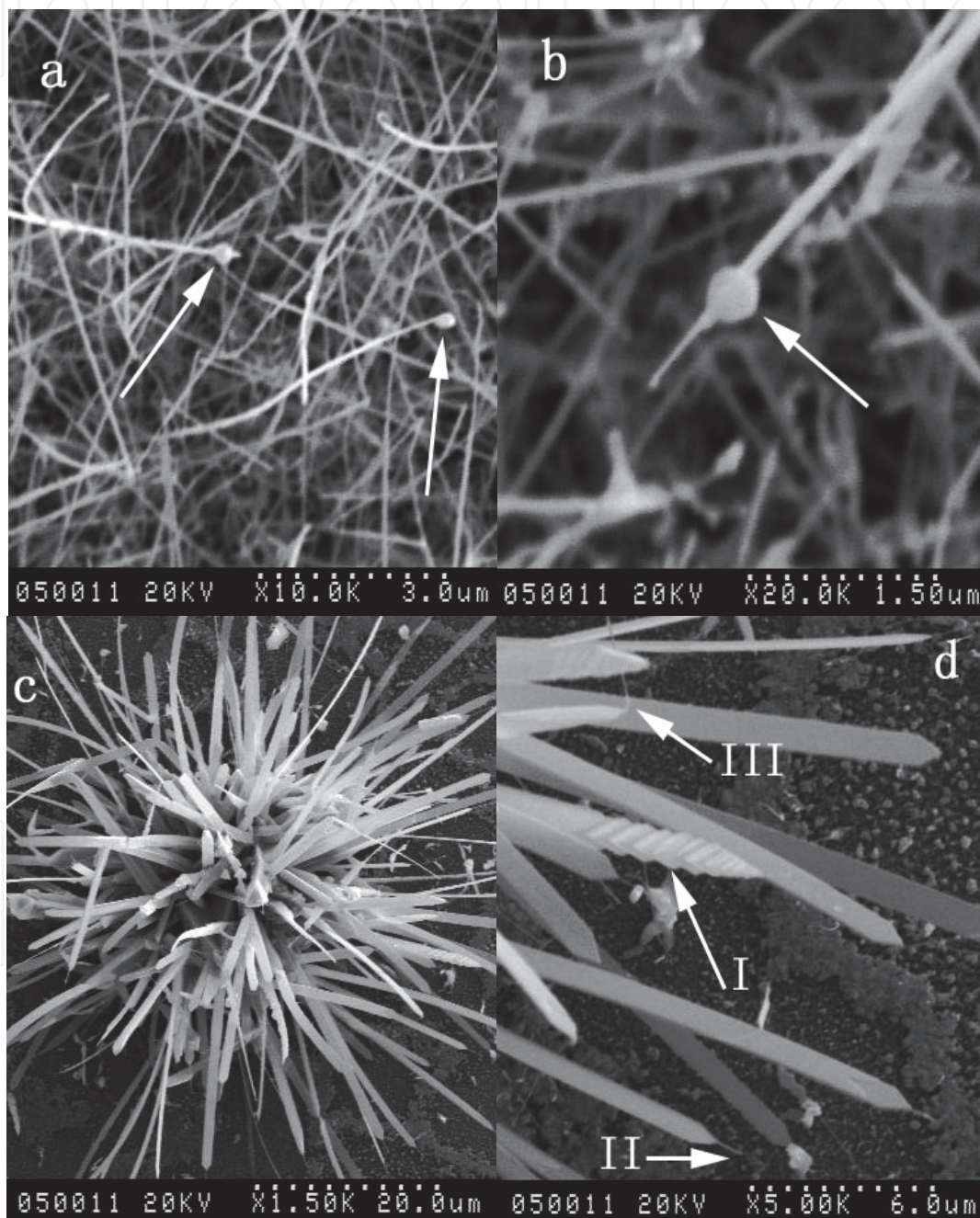


Fig. 17. SEM images of the sample catalyzed by 20 nm MgO thin film as intermediate layer and ammoniated at different temperatures. a, 950 °C; b, 1000 °C; c, 1050°C; d, enlarged picture at the limbic part of c.

As shown as Figure 17, nanoparticles exist on the tips of the GaN nanowires, which shows that the growth mechanism complies with vapor-liquid-solid (VLS) process. Grown at 950 °C, nanowires occur, grown at 1000 °C, nanorods exist, and when the ammoniating temperature increase to 1050 °C, nanobelts appear. That is, the ammoniating temperatures can affect the morphology of the GaN samples deeply.

Figure 18 show HRTEM and SAED images of an individual nanowire with MgO as intermediate layer.

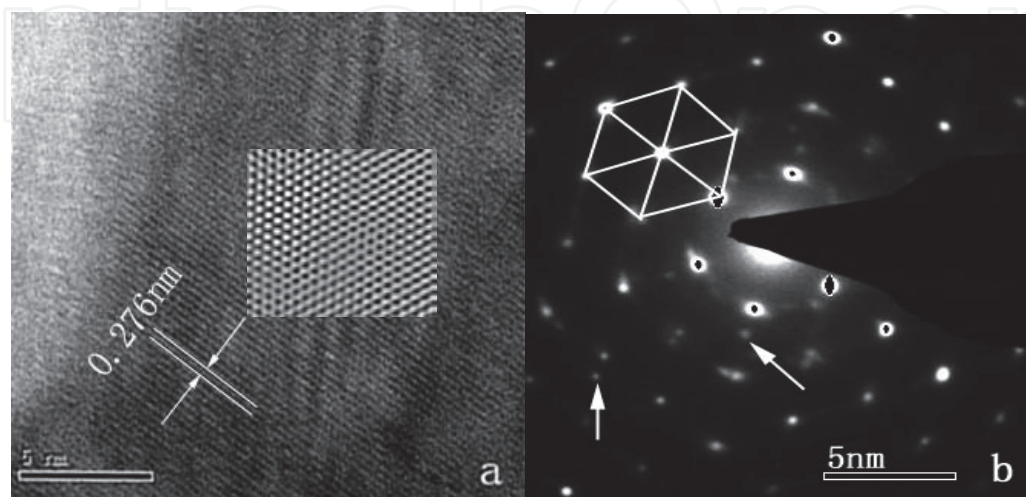


Fig. 18. (a) HRTEM, (b) SAED images of an individual nanowire with MgO as intermediate layer. The inset picture in HRTEM is a two-dimensional crystals space picture from rapid Fourier inverse transformation of image a.

Figure 18 indicate that GaN nanowire can form when MgO was used as intermediate layer with high crystalline quality. The crystal plane spacing of nanowire is about 0.276 nm, which corresponds to (100) crystal plane spacing (0.276 nm) of hexagonal GaN single crystal. No defects are observed.

Different compounds ( $C_m$ ) have great influence on the optical properties of GaN nanowires. We summarized the data after testing all the samples catalyzed by  $Al_2O_3$ , ZnO, SiC, and BN, which are listed in Table 2.

$Al_2O_3$	ZnO	SiC	BN
347 nm	344 nm	371 nm	373 nm

Table 2. Wavelengths of strong UV emission peaks for the samples catalyzed by different  $C_m$ .

As shown in Table 2, the wavelengths could be shorten when oxidizing materials were used as intermediate layers, i.e., blue-shift, while when carbide and nitride were used as intermediate layers, the wavelengths could increase, i.e., red-shift.

### 2.2.3 Summary

GaN can grow along preferred (002) planes catalyzed by  $Al_2O_3$  (10 nm), ZnO (20 nm), and  $TiO_2$  (30 nm), which were fabricated at the optimal conditions. However, other samples can't grow along preferred (002) planes.

Pure and clear GaN nanostructures can be formed with ZnO, MgO, and BN as intermediate layers. GaN nanowires are formed with ZnO, and BN as intermediate layers, and nanobelts

are formed with MgO, as intermediate layers. When the thickness of ZnO increases from 20 nm to 200 nm, the sample can turn from GaN nanowires to nanorods. The ammoniating temperatures can affect the morphology of the GaN samples deeply. Nanowires occur at 950 °C, nanorods exist at 1000 °C, nanobelts appear at 1050 °C.

The wavelengths (PL spectra data) could be shortened when oxidizing materials were used as intermediate layers, i.e., blue-shift, while when carbide and nitride were used as intermediate layers, the wavelengths could increase, i.e., red-shift.

### 2.3 Mg-Doped GaN nanowires

To improve the progress in GaN-based nano-photoelectric device and to enhance photoelectric performance of nano-devices, proper doping is very necessary. P-type doping and p-n junctions are great significance in fabricating nanowires (Fasol,1996; Nakamura,1998) and the formation of p-typed GaN films is the key technology in developing these devices and p-doping of GaN nanostructures with Mg as dopant is more effective in practice than with other dopants, because the ionic radius of Mg (0.65Å) is only slightly greater than that of Ga (0.62Å), and the gallium positions can be easily substituted by Mg under certain conditions. In this work, Mg-doped GaN nanowires were synthesized by a technique resembling the delta-doping method, and the concentration of Mg in GaN nanowires was varied to study its influence on the surface morphology, crystallinity, and optical properties of Mg-doped GaN nanowires (Shi et al., 2010a; Zhang et al., 2009).

#### 2.3.1 Experimental procedures

Mg-doped GaN nanowires have been fabricated using ammoniating Ga<sub>2</sub>O<sub>3</sub> films doped with Mg under flowing ammonia atmosphere. First, the Mg doped Ga<sub>2</sub>O<sub>3</sub> films were grown on Si (111) substrates by sputtering the Mg target of 99.99% purity and the sintered Ga<sub>2</sub>O<sub>3</sub> target of 99.999% purity in a JCK-500A radio frequency magnetron sputtering system. Both the Mg target and Ga<sub>2</sub>O<sub>3</sub> target were subjected to direct-current (DC) and radio-frequency (RF) magnetron sputtering, respectively. Next 30 cycles of this process were performed for a total deposition time of about 100 min, after which the total thickness of the Mg-doped Ga<sub>2</sub>O<sub>3</sub> films was about 630 ~ 850 nm. In a single sputtering cycle, first an undoped Ga<sub>2</sub>O<sub>3</sub> layer of 6 ~ 30 nm in thickness was deposited, followed by an approximately 5 nm Mg buffer layer. Figure 19 shows the growth sketch of the Ga<sub>2</sub>O<sub>3</sub> films.

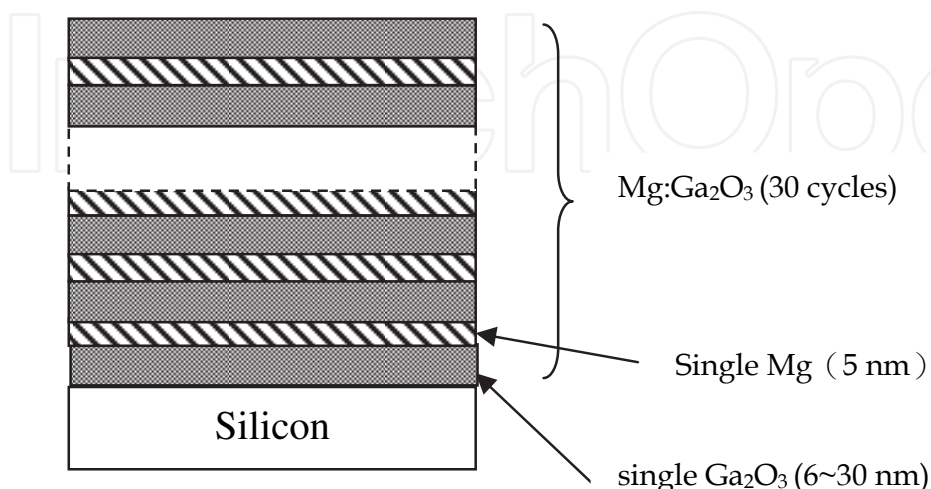


Fig. 19. The growth sketch of the Mg doped Ga<sub>2</sub>O<sub>3</sub> films.

Second, the  $\text{Ga}_2\text{O}_3$  thin films as deposited were ammoniated at  $\text{NH}_3$  atmosphere in a conventional tube furnace at 850 °C, 900 °C, and 950 °C for 5 min, 10 min, 15 min, and 20 min, respectively. The working conditions were, 150-Watt RF sputtering power of 13.56 MHz ; 20-Watt DC sputtering power; background pressure of  $0.9 \times 10^{-3}$  Pa; and pure Ar ( $\geq 99.99\%$ ) as the working at a working pressure of 2 Pa.

### 2.3.2 Results and discussion

Figure 20, and 21 show the X-ray diffraction patterns of the samples grown at 850 °C, 900 °C, and 950 °C for 15 min.

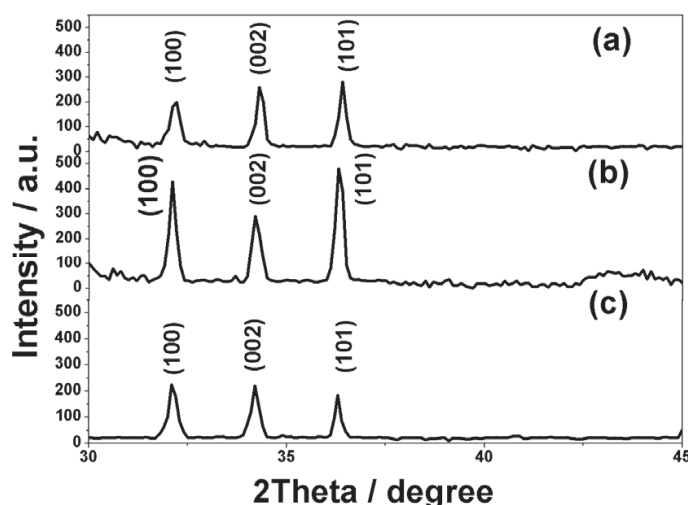


Fig. 20. X-ray diffraction patterns of samples at different temperature for 15 min, (a) 850 °C; (b) 900 °C; (c) 950 °C.

As shown in Figure 20, the samples following ammoniation are hexagonal wurtzite GaN (JCPDS card No.65-3410, International Center for Diffraction Data, 2002) with lattice constant of  $a = 0.3186$  nm and  $c = 0.5178$  nm, with the diffraction peaks located at  $2\theta = 32.1^\circ$ ,  $34.2^\circ$  and  $36.4^\circ$  corresponding to (100), (002) and (101) planes, which are consistent with the reported values for bulk GaN. No peak of  $\text{Ga}_2\text{O}_3$ , Mg or MgO is observed, indicating that neither  $\text{Ga}_2\text{O}_3$ , Mg metal nor MgO coats the nanowire surface.

The intensity of the sample shown in Figure 20b is stronger than that of the samples ammoniated at 850 °C and 950 °C, which shows the highest crystalline quality of this sample. The diffraction peak intensities decrease when the ammoniation temperature is lower or higher than 900 °C, which is probably caused by incomplete growth of GaN grains at lower temperature and decomposition or sublimation of GaN grains at higher temperature (Yang et al., 2002).

Figure 21 show the X-ray diffraction patterns of the samples grown at 900 °C for 5 min, 10 min, 15 min, and 20 min, respectively.

As seen in Figure 21, the main phase of samples following ammoniation are hexagonal wurtzite GaN with lattice constant  $a = 0.3186$  nm and  $c = 0.5178$  nm, with the diffraction peaks located at  $2\theta = 32.1^\circ$ ,  $34.2^\circ$ , and  $36.4^\circ$  corresponding to (100), (002) and (101) planes, which are consistent with the reported values for bulk GaN. No peak of  $\text{Ga}_2\text{O}_3$ , Mg or MgO is observed, indicating that neither  $\text{Ga}_2\text{O}_3$ , Mg metal nor MgO coats the nanowire surface.

Crystalline increases gradually with the increase of ammoniating time from 5 min to 15 min, and reaches the strongest intensity for the diffraction peak at 15 min, then decreases at 20 min, which is probably caused by incomplete reaction at less time and decomposition or sublimation at more time.

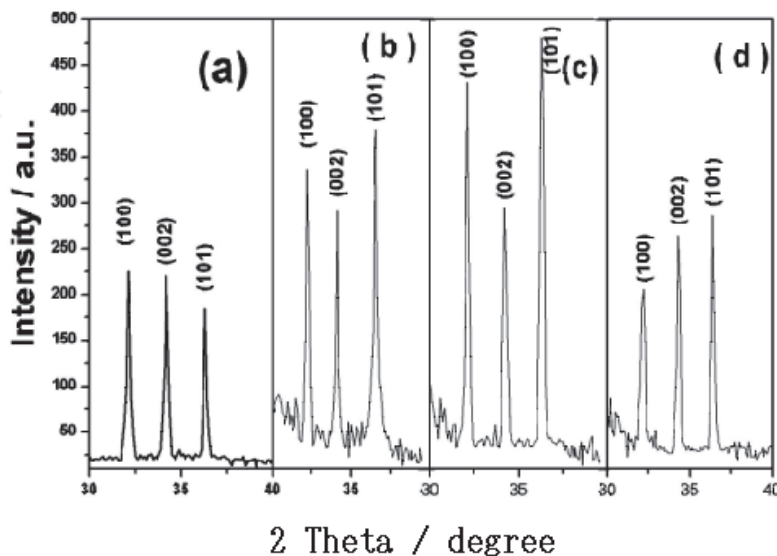


Fig. 21. X-ray diffraction patterns of samples at 900 °C for different time, (a) 5 min; (b) 10 min; (c) 15 min; (d) 20 min.

To further analyze the components of the GaN sample, FT-IR test was carried out for the sample after ammoniated at 900 °C for 15 min, as shown in Figure 22.

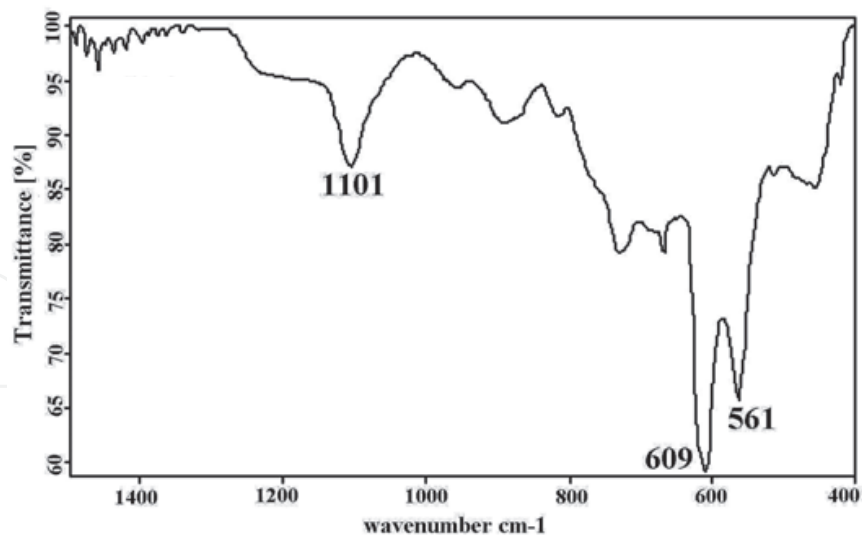


Fig. 22. FTIR pattern of the sample ammoniated at 900 °C for 15 min.

As seen in Figure 22, there are three well-defined prominent absorption bands, located at 561  $\text{cm}^{-1}$ , 609  $\text{cm}^{-1}$ , and 1101  $\text{cm}^{-1}$ . The band at 561  $\text{cm}^{-1}$  corresponds to Ga-N stretching vibration in hexagonal type GaN crystal, and the other bands correlate to the Si substrate. The peak at 609  $\text{cm}^{-1}$  is associated with the local vibration of substituted carbon in the Si crystal lattice (Sun et al., 1998) whereas the band at 1101  $\text{cm}^{-1}$  is attributed to the Si-O-Si

asymmetric stretching vibration because of the oxygenation of the Si substrate. There is no Ga-O bond or other absorption band in the spectrum; therefore,  $\text{Ga}_2\text{O}_3$  films react with  $\text{NH}_3$  completely at  $900^\circ\text{C}$  and form the hexagonal-type GaN crystal, which is the same as the results of the XRD.

The sample was also characterized by XPS as shown in Figure 23.

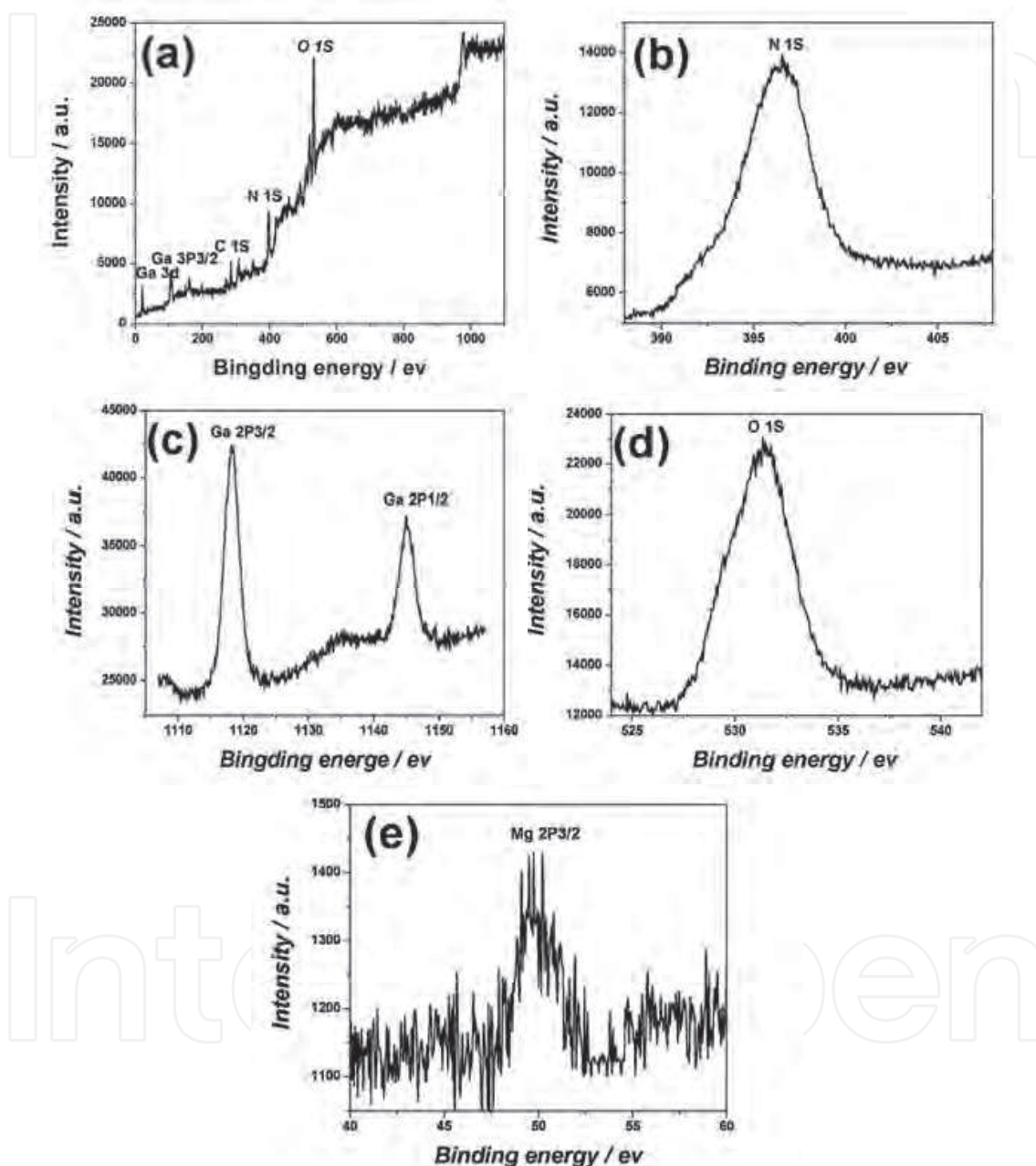


Fig. 23. XPS spectrum of the sample ammoniated at  $900^\circ\text{C}$  for 15 min, (a) general scan spectrum; (b) N1s band; (c)  $\text{Ga}2p_{1/2}$  and  $\text{Ga}2p_{3/2}$  band; (d) O1s band; (e)  $\text{Mg}2p_{3/2}$  band.

Figure 23a shows the XPS images of N1s, Ga2p, Ga3d, and O1s for GaN synthesized at the ammoniating temperature of  $900^\circ\text{C}$ , respectively. Figure 23a shows the general scan in the binding energy, ranging from 0 eV to 1100 eV with the main components being Ga, C, N, and O, with XPS peaks at the location of Ga3d (20.1 eV), Ga3p (109.1 eV), Ga3s (167.3 eV),

C1s (288.3 eV), N1s (397.6 eV) and O1s (534.3 eV). The strong peak at the site of 189.6 eV is LMM Auger peak of Ga element. C and O arise from the surface pollution of the sample. As observed, the energy peak for N1s shown in Figure 23b is centered at 397.6 eV, instead of 399 eV (binding energy of N element existing as atomic style), similar to the results of Li (397.4 eV) and Veal (397.6 eV), that is, the N atom exists as a nitride. The width and slight asymmetry of the N1s peak are attributed to N-H<sub>2</sub> and N-H<sub>3</sub> formation due to the interaction between N<sub>2</sub> and NH<sub>3</sub> at the GaN film<sup>[18]</sup> surface.

As seen in Figure 23c, the core level of Ga has a positive shift from elemental Ga. This shift in the binding energies of Ga and N confirms the bonding between Ga and N and the absence of elemental gallium. The binding energies of Ga2p<sub>1/2</sub> and Ga2p<sub>3/2</sub> are 1145.0 eV and 1118.1 eV, respectively, which are consistent with the results reported by different references of Ga2p<sub>3/2</sub> (1117.4 eV) (Elkashaf et al., 1998), Ga2p<sub>1/2</sub> (1144.8 eV) (Kingsley et al., 1995), and Ga2p<sub>1/2</sub> (1144.3 eV) (Sasaki et al., 1998). No bond formation is observed between Ga and O as the Ga3d spectrum does not show any satellite peak corresponding to β-Ga<sup>[21]</sup>, but shows the Ga atom existing only as combined GaN, not Ga<sub>2</sub>O<sub>3</sub>.

The percentage of elements is calculated according to the formula (Choi et al., 1998) as follows.

$$X\% = \left( \frac{A_x}{S_x} \right) / \sum_{i=1}^N \frac{A_i}{S_i}$$

A<sub>x</sub> (A<sub>i</sub>) indicates the peak area of element, x (i); S<sub>x</sub> (S<sub>i</sub>) is the atomic sensitivity factor of x (i) element; N is the number of the total elements. The values of the atomic sensitivity factors of Ga and N atoms are 6.9 and 0.38, respectively. Therefore, quantification of the peaks shows that the atomic ratio of Ga to N is approximately 1:1.09.

As shown in Figure 23d, the O1s peak is centered at 530.9 eV. According to Amanullah *et al.*, generally, the O1s peak had been observed in the binding energy region of 529-535 eV, and the peak around 529 - 530 eV is ascribed to lattice oxygen. For chemisorbed O<sub>2</sub> on the surface, the binding energy ranged from 530.0 eV to 530.9 eV. Therefore, the O1s peak in the present work is part of chemisorbed oxygen.

Figure 23e indicates the Mg2P<sub>3/2</sub> peak is at the site of 49.3 eV, with the bonding energy of Mg (Zhang et al., 2009). The XPS results show that the sample is Mg-doped GaN, similar to that of the XRD (Zhang et al., 2009).

Figure 24 shows the typical SEM images of the samples grown at different temperatures.

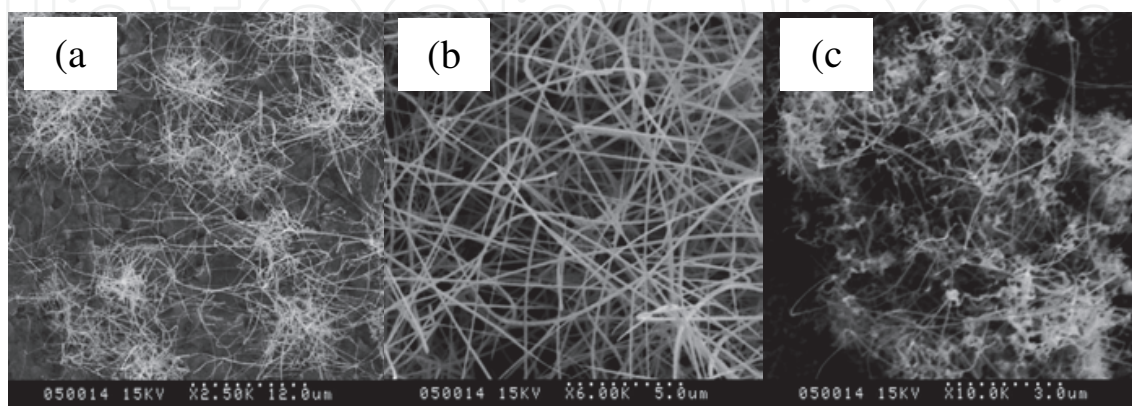


Fig. 24. SEM images of the samples grown at different temperatures, (a) 850 °C (b) 900 °C (c) 950 °C.

Figure 24a shows many cluster-like nanowires distributed on the sample surface, each of which grows radially outward, from the same point on the substrate. These nanowires are thin in diameter but rough on the surface, which are of 35 nm in diameter and 10-20  $\mu\text{m}$  in length. Figure 24b shows the sample comprises several one-dimensional nanowires distributed evenly on the substrate. As compared with the nanowires shown in Figure 24a, these one-dimensional nanowires have cleaner surfaces and are of greater quantity. Most of which are straight and smooth, uniformly thick along the spindle direction, and they intertwine with each other, possessing a thicker diameter of 50 nm and a longer length of several tens of microns. In Figure 24c, a large number of gossypine nanostructures are clearly observed, because of decomposition or sublimation of GaN grains at higher temperature, however, the amount of the GaN nanowires decrease, comparing with the sample shown in Figure 22b.

Ammoniating temperature has great influence on the morphology of the GaN nanowires and with the increase in ammoniating temperature from 850  $^{\circ}\text{C}$  to 900  $^{\circ}\text{C}$  (Shi et al., 2011), the diameter, the length, and the quantity increase but their quantity and crystallinity decrease when the ammoniating temperature rises to 950  $^{\circ}\text{C}$ . The GaN grains can't crystallize completely at lower temperature of 850  $^{\circ}\text{C}$ , however, the samples can decomposition or sublimation at higher temperature of 950  $^{\circ}\text{C}$ . In short, the crystalline is at its best after ammoniation at 900  $^{\circ}\text{C}$ , from the observation shown in Figure 24.

Figure 25 shows the typical SEM images of the samples at 900  $^{\circ}\text{C}$  for different times.

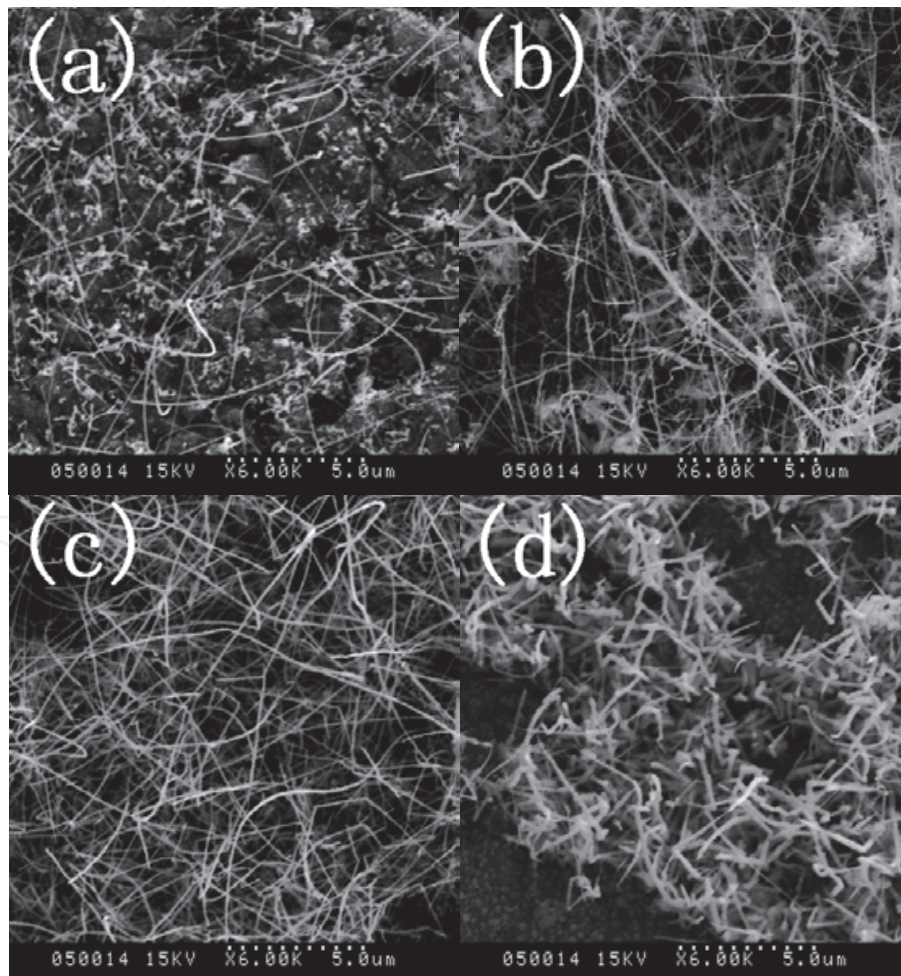


Fig. 25. Typical SEM images of the samples at 900  $^{\circ}\text{C}$  for 5 min, 10 min, 15 min, 20 min.

As shown in Figure 25a, most  $\text{Ga}_2\text{O}_3$  thin film has been ammoniated after ammoniated at 5 min. There are many irregular nanoparticles covered on the substrate surface with a small amount of nanowires. These nanowires interwine with each other and distribute on the surface randomly having the size of 35 nm in diameter and less than ten microns in length. Clear variation occurs on the surface of the samples, observed from Figure 25b, Figure 25c and Figure 25d. When ammoniated at 10 min, substrate surface is covered by nanowires completely but they are uneven thickness with 10-20 microns. Figure 25c shows nanowires become smooth and clean with even diameter of about 50 nm and 20 microns in length, while in Figure 25d, the nanowires become shorter and thicker with coarse surface, which is because of recrystallization of GaN. The results are consistent with XRD analysis. Ammoniating time has great influence on the morphology of the GaN nanowires and the nanowires become more in number, longer in length, and thicker in diameter with the increase of ammoniating time. The GaN grains can't crystallize completely at shorter time of 5 min and 10 min, however, the samples can recrystallize at longer time of 20 min. In short, the crystalline is at its best after ammoniation for 15 min from the observation of Figure 25.

Figure 26 shows the TEM, SAED, HRTEM and EDX images of an individual nanowire grown at 900 °C for 15 min.

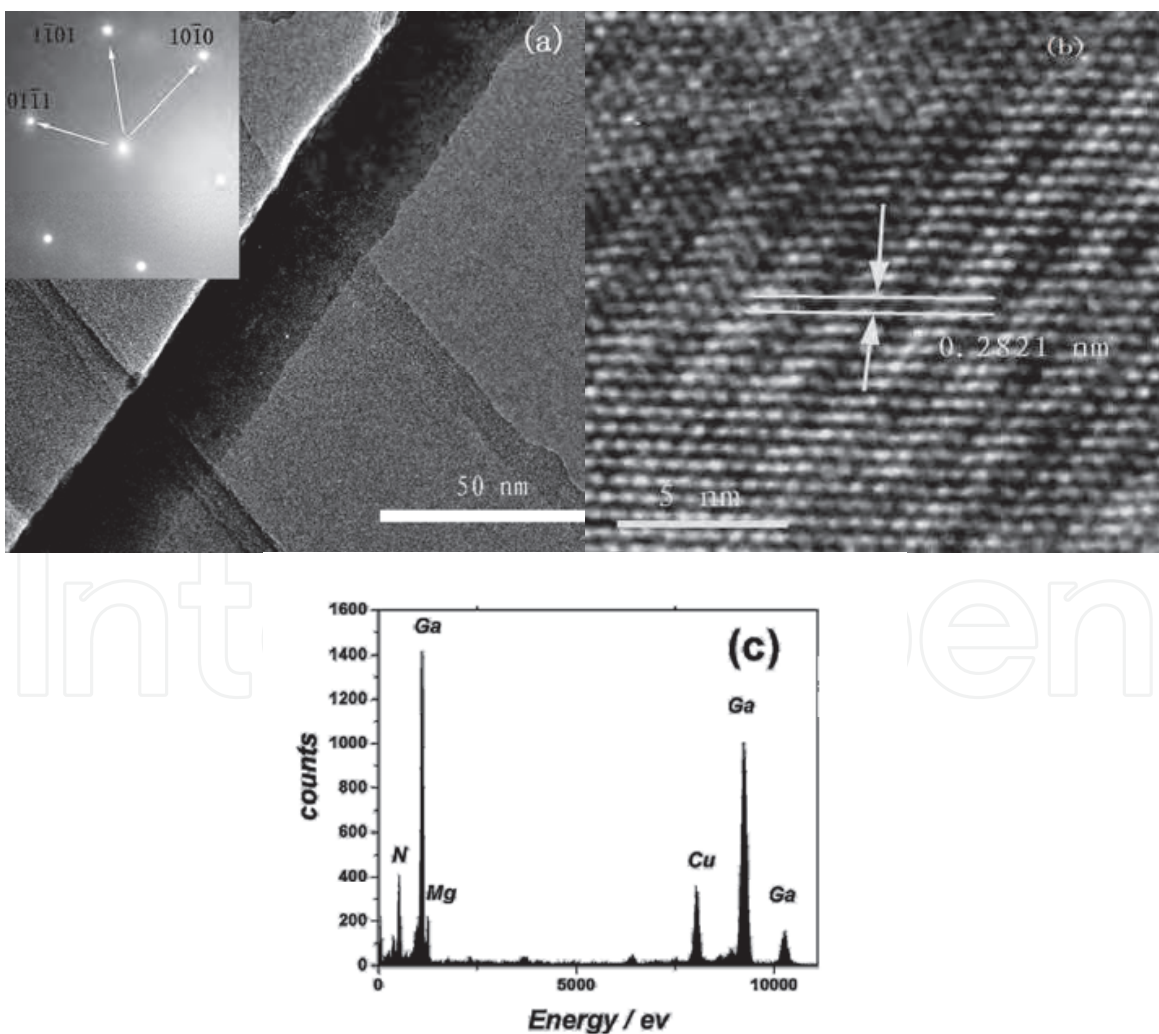


Fig. 26. TEM, SAED, HRTEM and EDX images of individual nanowire.

Figure 26a shows that the nanowire is 35 nm in diameter with a coarse surface. The reason for the coarse surface is attributed to the decreased mass transportation of Ga affected by the rich N atmosphere and Mg doping during growth<sup>[26]</sup>. Diffraction spots from SAED (the inset in Figure 26a) are regular and correspond to the diffraction zone axis of  $[1\bar{2}1\bar{3}]$ , which reveals the GaN nanowire is monocystal with a hexagonal wurtzite structure.

Seen from Figure 26b, the HRTEM lattice image of the straight GaN nanowire and the well-spaced lattice fringe in the image indicate the single crystal structure of GaN nanowires with high crystalline quality but with less dislocations and defects. The crystal plane spacing of nanowires is about 0.2821 nm, which is larger than that of (100) crystal plane spacing (0.2757 nm) of the hexagonal GaN single crystal. Mg doping slightly changes the lattice constant of GaN. The growth direction of this nanowire is parallel to  $[100]$  the orientation. Figure 26c shows the EDX image of this nanowire and reveals its composition as follows, 47% Ga, 48.5% N and 3% Mg (mole fraction), which is similar to that of the XPS (Shi et al., 2010a).

Figure 27 is the photoluminescence spectrum of samples ammoniated at 900°C for different time, detected with He-Cd laser used as the excitation source (with a wave length of 325 nm) at room temperature.

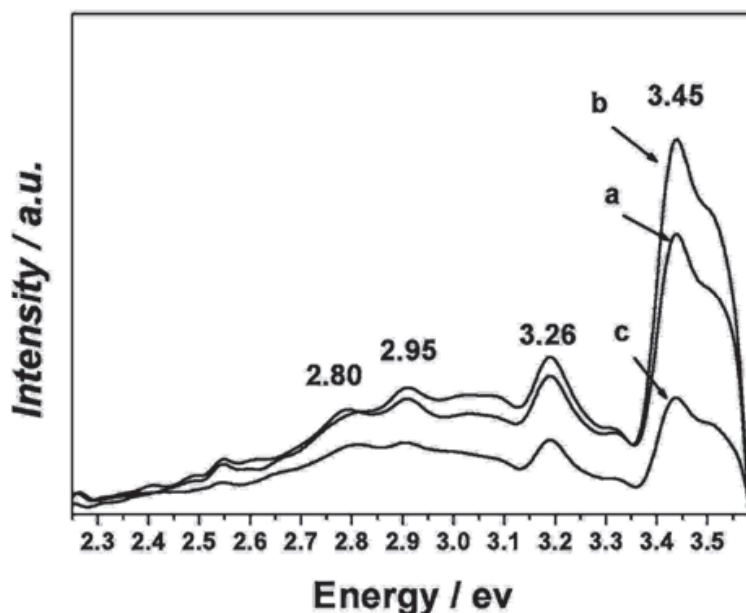


Fig. 27. Photoluminescence spectrum of samples ammoniated at 900°C for different times; (a) 10 min; (b) 15 min; (c) 20 min.

According to Figure 27, the nanowires show four emission peaks, their corresponding  $E_v$  are 3.45 eV, 3.26 eV, 2.95 eV, and 2.80 eV, respectively. A clear blueshift of the band-gap emission has occurred, from 3.39 eV for bulk GaN to 3.45 eV for Mg-doped GaN. When GaN is doped with Mg, the excess carriers generated enter to the conduction band of GaN and effectively hinder the transition of electrons at the bottom of GaN conduction band, thereby increase the energy from the conduction band to the valence band when electrons excited. This leads to a blueshift in the optical band-to-band transitions. This is consistent with the Burstein-Moss effect (Zhou et al., 2004). As for the emission peak at 3.26 eV, it is caused by the transition of electrons from the bottom of GaN conduction band to shallow acceptor level of Mg (acceptor level of Mg is at the site of 200 meV above valence band). The

emission bands at the site of 2.95 eV and 2.80 eV are caused by deep acceptor level of Mg doping. This observation consists with the results of Zolper et al (Zolper et al., 1996). The sites of the four emission peaks do not change but the strength of the emission peaks changes obviously with the increase of ammoniating time. Ammoniating time has great influence on the optical properties and the best condition is 15 min.

Figure 28 is the photoluminescence spectrum of samples ammoniated at different temperatures for 15 min, detected with He-Cd laser used as the excitation source (with a wave length of 325 nm) at room temperature.

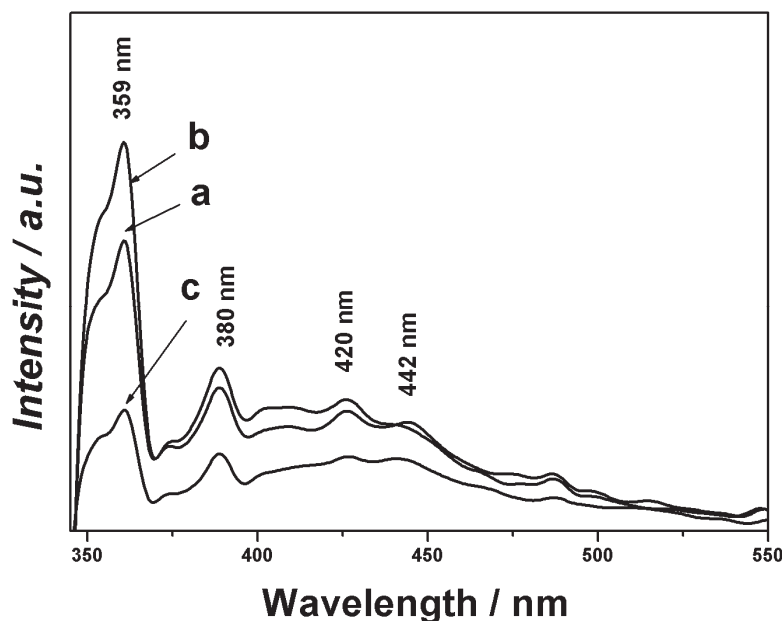


Fig. 28. Photoluminescence spectrum of samples ammoniated at different temperatures for 15 min. (a) 850 °C; (b) 900 °C; (c) 950 °C.

The nanowires show four emission peaks, at 359 nm, 380 nm, 420 nm, and 442 nm. Bulk GaN shows photoluminescence at 365 nm at room temperature. According to the equation  $E_v/\text{eV} = 1240/\lambda$ , the peak at 359 nm corresponds to  $E_v = 3.45$  eV. Thus, a clear blueshift of the band-gap emission has occurred, too. The reason is just like what has stated above. The other three peaks located at 380 nm, 420 nm, and 442 nm correspond to 3.26 eV, 2.95 eV, and 2.80 eV, respectively, and can be explained the same as that in Figure 10. The sites of the four emission peaks do not change but the strength of the emission peaks changes obviously with the variation of ammoniating temperature, which indicates the optical properties are closely related to ammoniating temperature. The luminous intensity of GaN nanostructures is at its best at 900°C.

### 2.3.3 Growth mechanism

During the nanowire growth process, higher surface energy exist on the nanowire's tip, but lower surface energy exist on their sides. The sides of the nanowires play a significant role during the growth process as a path to provide materials. The main aim of GaN molecules, Ga atoms, and N atoms is to find a position with higher surface energy and to grow there so as to decrease the surface energy.

Mg metal and Si element can react and form silico-magnesium alloys, which exist as a dissociative phase. The silico-magnesium alloys can not only promote the growth of the GaN nanowires and the chemical reaction, but also inevitably lead to the uneven distribution of the energy on the substrate surface, i.e., some positions have high surface energy and the energy can aggregate around the defects, thus providing nucleation points for the GaN nanowires (Shi et al., 2010c).

Cluster-like GaN nanowires are seen on the Si substrate surface, as identified in Figure 29.

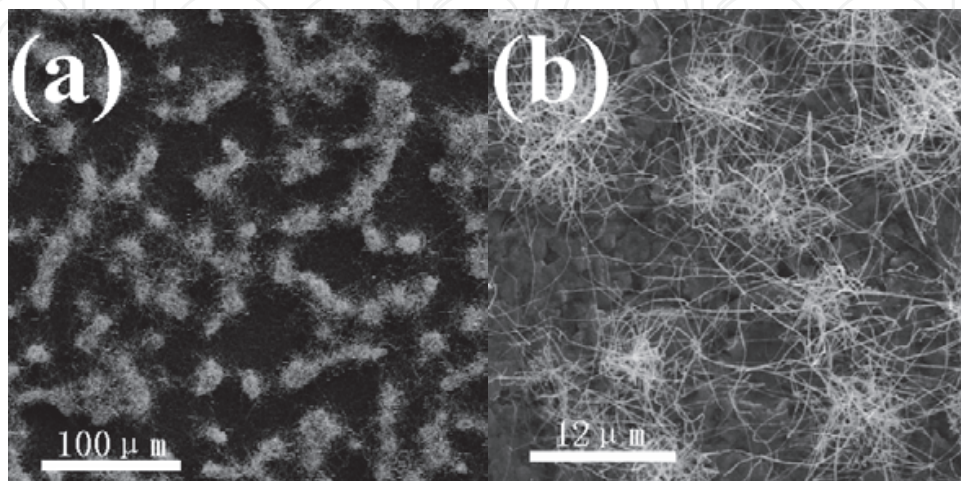


Fig. 29. SEM images of the cluster-like nanowires distributed on Si substrate surface, an ordinary area of substrate and (b) the amplified image of sample (a).

More defects exist on the Si substrate surface, i.e., aggregation of the defect energy, which have more broken bonds and lower chemical power. Therefore, the GaN nanowires will grow at the sites of the defects, the aggregation sites of the defect energy become the nucleation points for the GaN nanowires, as shown in Figure 30.

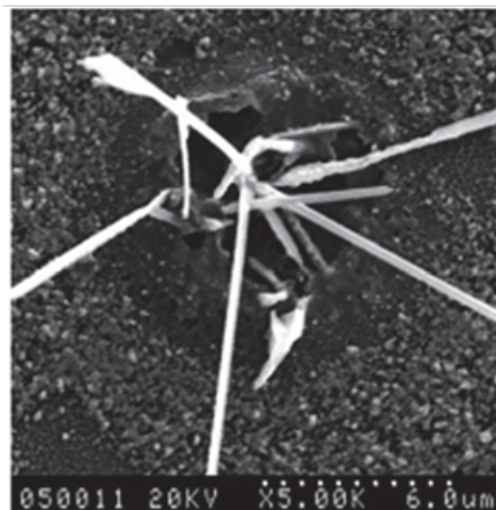


Fig. 30. SEM image of a defect on the Si substrate surface and the nanostructure growth from this position with more energy aggregated.

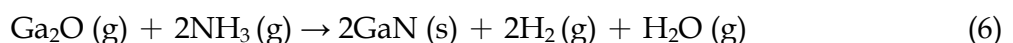
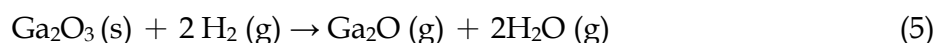
In the sputtering process, a multilayer structure of Mg-doping  $\text{Ga}_2\text{O}_3$  films is obtained. Thus, Mg has greater opportunity to substitute Ga, and then leads to more defects. In the

annealing process,  $\text{NH}_3$  decomposes into  $\text{NH}_2$ ,  $\text{NH}$ ,  $\text{H}_2$ , and  $\text{N}$ , when the ammoniating temperature reaches  $850^\circ\text{C}$ . The Ga atoms can combine with the N atoms, and  $\text{Ga}_2\text{O}$  can react with  $\text{NH}_3$  to form GaN molecules, and finally form GaN microcrystallites. These microcrystallites become the seed crystals for the GaN nanowires growth.

GaN molecules carried by air flow would combine with the GaN microcrystallites and induce the GaN microcrystallites' growth. There are broken bonds on the GaN nanostructure surfaces, and the defect energy can aggregate together so that the Ga atoms and N atoms can be absorbed from the surrounding saturated gas by the broken bonds of the defects to form a Ni-Ga-N structure. The absorbed Ga and N atoms could also generate broken bonds, therefore, the absorption process could carry on continuously. However, when the concentration of gas reduces or when the defect energy of the nanowires falls to a level that is insufficient to absorb Ga- and N atoms, the growth of the GaN nanowires can stop at last.

As seen from a macro-perspective, the formation of the GaN nanowires included absorption, migration, nucleus formation, aggregation, growth and desorption before they turn to GaN nanowires. Meanwhile, Mg is doped into the GaN cells to occupy the Ga vacancies because the ion radius of Mg (0.065 nm) is similar to that of Ga (0.062 nm). Mg doping can distort the GaN cell, which can introduce more defects, so the defect energy increases, which promotes the growth of the GaN nanowires. This theory can be called "defect energy confinement theory" (Shi et al., 2010c).

The reaction formula of  $\text{Ga}_2\text{O}_3$  becoming GaN are as follows:



Therefore, we think that the H atoms decomposed from  $\text{NH}_3$  can promote the decomposition of  $\text{Ga}_2\text{O}_3$  to generate more Ga atoms and  $\text{Ga}_2\text{O}$  molecules; then Ga atoms and  $\text{Ga}_2\text{O}$  molecules can react with N atoms to form GaN, which is decomposed from  $\text{NH}_3$ . That is, the growth mechanism complies with vapor-liquid-solid (VLS) process and the aggregation of the defect energy accelerates this growth of the GaN nanowires.

#### 2.3.4 Summary

The predominant phase of the samples fabricated by the magnetron sputtering method is the hexagonal wurtzite GaN crystal identified by the XRD analysis. The best condition to fabricate the GaN nanowires is at  $900^\circ\text{C}$  for 15 min, the highest crystalline quality can be obtained at this condition. The presence of the Ga-N bond is established by the FTIR spectrum and the N atom exists as a nitride by XPS and quantification of the peaks reveals that the atomic ratio of Ga to N is approximately 1:1.09.

Ammoniating temperatures and ammoniating times greatly influence the GaN nanowires morphology. The GaN nanowires grown at  $900^\circ\text{C}$  for 15 min are straight and smooth with uniform thickness along the spindle direction, 50 nm in diameter and several tens of microns in length, with high crystalline quality. The growth direction of this GaN nanowire is parallel to [100] orientation.

PL spectra show that GaN nanowires after ammoniation at  $900^\circ\text{C}$  for 15 min possess good optical properties and have a strong emission peak at 359 nm. The optical properties of the

GaN nanowires are closely related to the ammoniating temperature and ammoniating time, because the strength of the emission peak changes with the variation in temperature and time, whereas its site does not change accordingly.

The aggregation of the defect energy is used to explain the growth mechanism of the GaN nanowires. Mg doping causes the distortion of the GaN cell and introduces more defects in the crystal cell so that the defect energy are added, which promotes the growth of the GaN nanowires. The growth mechanism mainly follows the VLS process, and the aggregation of the defect energy accelerates this growth of the GaN nanowires.

### 3. Conclusion

#### 3.1 Catalyzed by $M_e$

We have been fabricated large-scale single-crystalline GaN nanowires with high-quality by RF magnetron sputtering method using Ti, V, Cr, Co, Nb, Mo, Ta, and Tb ( $M_e$ ) as catalysts.

The diameters increase with the number of the protons, for example, the samples can form GaN nanowires when catalyzed by Ti, V, and Cr, however, with the increase in the protons, nanorods can be formed, such as the sample catalyzed by Co. As for V, Nb, and Ta, which are of the same sub-group, nanowires can be formed catalyzed by V, however, nanorods can be formed when catalyzed by Nb and Ta. Cr and Mo are of the same subgroup, the sample catalyzed by Cr can form nanowires, while after catalyzing by Mo, nanorods can be formed. That is, the catalytic action increases with the increase in the number of the protons at the same line of the Periodic Table of chemical elements, with the morphology becoming obvious. And the same law exists in the same row.

GaN nanowires have good optical properties, which can be tested by PL spectra. The optical properties of GaN nanowires greatly depend on the ammonating temperatures and times. With the increase in the number of protons, the wavelength of the samples catalyzed by different elements can change their sites, i.e., blue-shift, red-shift, and then blue-shift, red-shift. In short, wavelength shifts to long wave, i.e., red-shift, with the increase in the number of the protons at the same line of the Periodic Table of chemical elements. While as for the same subgroup elements, from V to Nb to Ta, wavelength decreases, i.e., blue-shift. However, Cr is an exception, and the reason is unknown.

The growth procedure follows the VLS mechanism, and  $M_e$  acts as the nucleation point for GaN crystalline nuclei and plays an important role as catalyst during ammonation process. Defect energies confinement theory can also be applied to explain the formation of GaN nanostructures.

#### 3.2 Catalyzed by $C_m$

We have been fabricated large-scale single-crystalline GaN nanowires with high-quality by RF magnetron sputtering method using MgO, TiO<sub>2</sub>, Al<sub>2</sub>O<sub>3</sub>, SiC, BN, and ZnO (short for  $C_m$ ) as intermediate layers. GaN can grow along preferred (002) planes catalyzed by Al<sub>2</sub>O<sub>3</sub> (10 nm), ZnO (20 nm), and TiO<sub>2</sub> (30 nm), which were fabricated at the optimal conditions. However, other samples can't grow along preferred (002) planes.

Pure and clear GaN nanostructures can be formed with ZnO, MgO, and BN as intermediate layers. GaN nanowires are formed with ZnO, and BN as intermediate layers, and nanobelts are formed with MgO, as intermediate layers. When the thickness of ZnO increases from 20

nm to 200 nm, the sample can turn from GaN nanowires to nanorods. The ammoniating temperatures can affect the morphology of the GaN samples deeply. Nanowires occur at 950 °C, nanorods exist at 1000 °C, nanobelts appear at 1050 °C.

The wavelengths (PL spectra data) could be shortened when oxidizing materials were used as intermediate layers, i.e., blue-shift, while when carbide and nitride were used as intermediate layers, the wavelengths could increase, i.e., red-shift.

### 3.3 Doped with Mg

Mg-doped GaN nanowires have been successfully grown on Si (111) substrates by magnetron sputtering through ammoniating Ga<sub>2</sub>O<sub>3</sub>/Mg thin films.

The aggregation of the defect energy is used to explain the growth mechanism of the GaN nanowires. Mg doping causes the distortion of the GaN cell and introduces more defects in the crystal cell so that the defect energy is added, which promotes the growth of the GaN nanowires. The growth mechanism mainly follows the VLS process, and the aggregation of the defect energy accelerates this growth of the GaN nanowires.

## 4. Acknowledgements

This project was supported by the Key Research Program of the National Natural Science Foundation of China (No.90201025) and the National Natural Science Foundation of China (No. 90301002). I also thank Prof. Cehngshan Xue for his great contribution to this project.

## 5. References

- Fasol, G. (1996). Room-Temperature Laser Diode Nitride Blue Gallium, *Science*, Vol. 272, No. 5269, (June 1996), pp. 1751-1752, ISBN 0036-8075
- Nakamura, S. (1998). The roles of structural imperfections in InGaN-Based blue light-emitting diodes and laser diodes, *Science*, Vol. 281, No. 5379, (August 1998), pp. 956-961, ISBN 0036-8075
- Morkoç, H.; Mohammad S.N. (1995). High-Luminosity Blue and Blue-Green Gallium Nitride Light-Emitting Diodes, *Science*, Vol. 267, No. 5194, (January 1995), pp. 51-55, ISBN 0036-8075
- Han, W.Q.; Fan, S.S.; Li, Q.Q. & Hu, Y.D. (1997). Synthesis of Gallium Nitride Nanorods Through a Carbon Nanotube-Confined Reaction, *Science*, Vol. 277, No. 5194, (August 1997), pp. 1287-1289, ISBN 0036-8075
- Lauhon, L.J.; Gudixsen, M.S.; Wang, D. & Lieber, C.M. (2002). Epitaxial core-shell and core-multishell nanowire heterostructures, *Nature*, Vol. 420, No. 6911, (November 2002), pp. 57-61, ISBN 0028-0836
- Ham, M.H.; Choi, J.H.; Hwang, W.; Park, C.; Lee, W.Y. & Myoung, J.M. (2006). Contact characteristics in GaN nanowire devices, *Nanotechnology*, Vol. 17, No. 9, (May 2006), pp. 2203-2206, ISBN 0957-4484
- Xu, B.S.; Zhai, L.Y.; Liang, J.; Ma, S.F.; Ja, H.S. & Liu, X.G. (2006). Synthesis and characterization of high purity GaN nanowires, *Journal of Crystal Growth*, Vol. 291, No. 1, (May 2006), pp. 34-39, ISBN 0022-0248

- He, M.; Minus, I.; Zhou, P.; Mohammed, S. N.; Halpern, J. B.; Jacobs, R.; Sarney, W. L.; Salamanca-Riba, L.; & Vispute, R. D. (2000). Growth of large-scale GaN nanowires and tubes by direct reaction of Ga with  $\text{NH}_3$ , *Applied Physics Letter*, Vol. 77, No.23, (December 2006), pp. 3731-3733, ISBN 0003-6951
- Xue, C.S.; Wei, Q.Q.; Sun, Z.C.; Dong, Z.H.; Sun, H.B. & Shi, L.W. (2004). Fabrication of GaN nanowires by ammoniating  $\text{Ga}_2\text{O}_3/\text{Al}_2\text{O}_3$  thin films deposited on Si(111) with radio frequency magnetron sputtering, *Nanotechnology*, Vol. 77, No.23, (July 2004), pp. 724-726, ISBN 0957-4484
- Li, J. Y.; Chen, X. L.; Qiao, Z.Y.; Cao, Y.G. & Lan, Y.C. (2000). Formation of GaN nanorods by a sublimation method, *Journal of Crystal Growth*, Vol. 213, No. 3-4, (June 2000), pp. 408-410, ISBN 0022-0248
- Shi, F.; Zhang, D.D. & C.S.Xue. (2010). Influence of Ammoniating Time on the Microstructure of Mg-Doped GaN Nanowires, *Materials Science and Engineerin: B*, Vol. 167, No. 1, (May 2010), pp. 80-84, ISBN 0921-5107
- Shi, F.; Li, H. & Xue, C.S. (2010). Fabrication of GaN nanowires and nanorods catalyzed with tantalum, *Journal of Materials Science: Materials in Electronics*, Vol. 21, No. 12, (December 2010), pp. 1249-1254, ISBN 0957-4522
- Perlin, P.; Jauberthie-Carillon, C.; Itie, J.P.; Miguel, A. S.; Grzegory, I. & Polian, A. (1992). Raman scattering and x-ray-absorption spectroscopy in gallium nitride under high pressure, *Physical Review B*, Vol. 45, No. 1, (January 1992), pp.83-89, ISBN 0163-1829
- Monemar, B. (1974). Fundamental energy gap of GaN from photoluminescence excitation spectra, *Physical Review B*, Vol. B10, No. 1, (July 1974), pp. 676-681, ISBN 1098-0121
- Yang, Y.G.; Ma, H.L.; Xue C.S., Zhuang, H.Z.; Hao, X.T.; Ma, J. & Teng, S.Y. (2002). Preparation and structural properties for GaN films grown on Si (111) by annealing, *Applied Surface Science*, Vol. 193, No. 1-4, (June 2002), pp. 254-260, ISBN 0169-4332
- Ai, Y.J.; Xue, C.S.; Sun, C.W.; Sun, L.L.; Zhuang, H.Z.; Wang, F.X.; Li, H. & Chen, J.H. (2007). Synthesis of GaN nanowires through  $\text{Ga}_2\text{O}_3$  films' reaction with ammonia, *Materials Letter*, Vol. 61, No. 13, (May 2007), pp. 2833-2836, ISBN 0167-577X
- Sun, Y.; Miyasato, T. S, & Nobuo. (1998). Outdiffusion of the excess carbon in SiC films into Si substrate during film growth, *Journal of Applied Physics*, Vol. 84, No. 11, (December 1998), pp. 6451-6453, ISBN 0021-8979
- Demichelis, F.; Crovini, G.; Pirri, C.F.; Tressoa, E.; Amatob, G.; Cosciac, U.; Ambrosonec, G. & Ravad, P. (1994). Optimization of a-Si<sub>1-x</sub>C<sub>x</sub>: H films prepared by ultrahigh vacuum plasma enhanced chemical vapour deposition for electroluminescent devices, *Thin Solid Films*, Vol. 241, No. 1-2, (April 1994), pp. 274-277 , ISBN 0040-6090
- Wei, Q.Q.; Xue, C.S.; Sun, Z.C.; Cao, W.T.; & Zhuang, H.Z. (2005). Formation of GaN Film by Ammoniating  $\text{Ga}_2\text{O}_3/\text{Al}_2\text{O}_3$  Deposited on Si(111) Substrate, *Rare Metal Materials and Engineering*, Vol. 34, No.2, (February 1994), pp. 312-315, ISBN 1002-185X

- Elkashaf, N.; Srinivasa, R.S.; Major, S. Sabharwal, S. C. & Muthec, K. P. (1998). Sputter deposition of gallium nitride films using a GaAs target, *Thin Solid Films*, Vol. 333, No.1-2, (November 1998), pp. 9-12, ISBN 0040-6090
- Kingsley, C.R.; Whitaker, T.J.; Wee, A.T.S.; Jackman, R. B. & Foord, J. S. (1995). Development of chemical beam epitaxy for the deposition of gallium nitride, *Materials Science and Engineering B*, Vol. 29, No.1-3, (January 1995), pp. 78-82, ISBN 0921-5107
- Sasaki, T. & Matsuoka, T. (1988). Substrate-polarity dependence of metal-organic vapor-phase epitaxy-grown GaN on SiC, *Journal of Applied Physics*, Vol. 64, No.9, (November 1988), pp. 4531-4535, ISBN 0021-8979
- Ishikawa, H.; Kobayashi, S.; Koide, Y.; Yamasaki, S.; Nagai, S.; Umezaki, J.; Koike, M.; & Murakami, M. (1997). Effects of surface treatments and metal work functions on electrical properties at *p*-GaN/metal interfaces, *Journal of Applied Physics*, Vol. 81, No.3, (February 1997), pp. 1315-1322, ISBN 0021-8979
- Li, D.; Sumiya, M.; Fuke, S. Yang, D.R.; Que, D.L.; Suzuki, Y. & Fukuda, Y. (2001). Selective etching of GaN polar surface in potassium hydroxide solution studied by x-ray photoelectron spectroscopy, *Journal of Applied Physics*, Vol. 90, No.8, (October 2001), pp. 4219-4223, ISBN 0021-8979
- Veal, T. D.; Mahboob, I.; Piper, L.F.J.; McConville, C. F. & Hopkinson, M. (2004). Core-level photoemission spectroscopy of nitrogen bonding in GaNAs alloys, *Applied Physics Letters*, Vol. 85, No.9, (August 2004), pp.1550-1552, ISBN 0003-6951
- King, S.W.; Carlson, E.P.; Therrien, R.J. Christman, J.A.; Nemanich, R. J. & Davis, R.F. (1999). X-ray photoelectron spectroscopy analysis of GaN/(0001) AlN and AlN/(0001) GaN growth mechanisms, *Journal of Applied Physics*, Vol. 86, No.10, (November 1999), pp. 5584-5593, ISBN 0021-8979
- Amanullah, F.M.; Pratap, K.J. & Hari, V.B. (1998). Compositional analysis and depth profile studies on undoped and doped tin oxide films prepared by spray technique, *Materials Science and Engineering B*, Vol. 52, No.2-3, (April 1998), pp.93-98, ISBN 0921-5107
- Xiao, H.D.; Ma, H.L.; Xue, C.S.; Hu, W.R.; Ma, J.; Zong, F.J.; Zhang, X.J. & Ji, F. (2005). Synthesis and structural properties of GaN particles from GaO<sub>2</sub>H powders, *Diamond and Related Materials*, Vol.14, No.10, (October 2005), pp.1730-1734, ISBN 0925-9635
- Bae, S.Y.; Seo, H.W.; Park, J.; Yang, H. & Kim, B. (2003). Porous GaN nanowires synthesized using thermal chemical vapor deposition, *Chemical Physics Letters*, Vol. 376, No.3-4, (July 2003), pp.445-451, ISBN 0009-2614
- Schlager, J.B.; Sanford N.A.; Bertness, K. A.; Barker, J. M.; Roshko, A. & Blanchard, P. T. (2006). Polarization-resolved photoluminescence study of individual GaN nanowires grown by catalyst-free molecular beam epitaxy, *Applied Physics Letters*, Vol. 88, No.21, (May 2006), pp.213106-213108, ISBN 0003-6951
- Chen, C.C.; Yeh, C.C.; Chen, C.H.; Yu, M.Y.; Liu, H.L.; Chen, K.H.; Chen, L.C.; Peng, J.Y. & Chen, Y.F. (2001). Catalytic Growth and Characterization of Gallium Nitride Nanowires, *Journal of the American Chemical Society*, Vol.123, No. 12, (February 2001), pp.2791-2798, ISBN 0161-4940

- Liu, H.L.; Chen, C.C.; Chia, C.T.; Yeh, C.C.; Chen, C.H.; Yu, M.Y.; Keller, S. & Nbaars, S. (2001). Infrared and Raman-scattering studies in single-crystalline GaN nanowires; *Chemical Physics Letters*, Vol.345, No.3-4, (September 2001), pp.245-251, ISBN 0009-2614
- Sun, Y.L.; Zhang, X.B.; Ning, Y.S.; Kong, F.Z. & Liu, F. (2002), CVD Method to Synthesize Carbon Nanotubes on a Large Scale, *Journal of Inorganic Materials*, Vol.17, No.2, (April 2002), pp.337-342, ISBN 1000-324X
- Wang, M.X.; Yang, L. & Wang, C.M.; (2004). Synthesis of One-Dimensional GaN Nanowires by Ammoniating, *Rare Metal Materials and Engineering*, Vol.33, No.6, (December 2004), pp.670-672, ISBN 1002-185X
- Ohno, Y.; Shirahama, T.; Takeda, S.; Ishizumi, A. & Kanemitsu, Y. (2005), Fe-catalytic growth of ZnSe nanowires on a ZnSe (001) surface at low temperatures by molecular-beam epitaxy, *Applied Physics Letters*, Vol. 87, No.4, (July 2005), pp. 043105-043107, ISBN 0003-6951
- Shi, F.; Wang, Z.P. & Xue, C.S. (2010). Synthesis and Characterization of GaN Nanowires through Ammoniating Ga<sub>2</sub>O<sub>3</sub>/Cr Thin Films Deposited on Si(111) Substrates, *Applied Surface Science*, Vol.256, No.16, (June 2010), pp.4483-4487, ISBN 0169-4332
- Tang, C.C.; Fan, S.S.; Dang, H.Y. ; Li, P. & Liu, Y. M.; (2000). Simple and high-yield method for synthesizing single-crystal GaN nanowires, *Applied Physics Letters*, Vol. 77, No.13, (September 2000), pp. 1961-1963, ISBN 0003-6951
- Xue, C.S.; Wu, Y.X.; Zhuang, H.Z.; Tian, D.H.; Liu, Y.-A.; Zhang, X.K., Ai, Y.J., Sun, L.L. & Wang, F.X. (2005). Growth and characterization of high-quality GaN nanowires by ammonification technique, *Physica E*, Vol. 30, No. 1-2, (December 2005), pp.179-181, ISBN 1386-9477
- Shi, F., Zhang, D.D. Xue, C.S. (2010). Influence of Ammoniating Time on the Microstructure of Mg-Doped GaN Nanowires, *Materials Science and Engineering B*, Vol.167, No.2, (May 2010), pp.80-84, ISBN 0921-5107
- Zhang, D.D.; Xue, C.S.; Zhuang, H.Z., Sun, H.B., Cao, Y.P., Huang, Y.L., Wang, Z.P. & Wang, Y. (2009). Influence of Mg Doping on GaN Nanowires, *Chemphyschem*, Vol.10, No.3, (February 2009), pp571-575, ISBN 1439-4235
- Choi, W.F.; Song, T.Y. & Tan, L.S. (1998), Infrared and X-ray photoelectron studies of as-prepared and furnace-annealed radio-frequency sputtered amorphous silicon carbide films, *Journal of Applied Physics*, Vol. 83, No.9, (May 1998), pp. 4968-4973, ISBN 0021-8979
- Shi F., Zhang, D.D. & Xue, C.S. (2011). Effect of ammoniating temperature on microstructure and optical properties of one-dimensional GaN nanowires doped with magnisum, *Journal of Alloys and Compounds*, Vol. 509, No.4, (January 2011), pp.1294-1300, ISBN 0925-8388
- Zhou, S.M.; Zhang, X.H.; Meng, X.M.; Zou, K.; Fan, X.; Wu, S.K. & Lee, S.T. (2004). The fabrication and optical properties of highly crystalline ultra-long Cu-doped ZnO nanowires, *Nanotechnology*, Vol. 15, No.9, (September 2004), pp.1152-1155, ISBN 0957-4484

Zolper, J.C.; Crawford, M.H.; Howard, A.J.; Ramer, J. & Hersee S.D. (1996). Morphology and photoluminescence improvements from high-temperature rapid thermal annealing of GaN, *Applied Physics Letters*, Vol. 68, No.2, (September 2000), pp. 200-202, ISBN 0003-6951

IntechOpen

IntechOpen



## **Nanowires - Fundamental Research**

Edited by Dr. Abbass Hashim

ISBN 978-953-307-327-9

Hard cover, 552 pages

**Publisher** InTech

**Published online** 19, July, 2011

**Published in print edition** July, 2011

Understanding and building up the foundation of nanowire concept is a high requirement and a bridge to new technologies. Any attempt in such direction is considered as one step forward in the challenge of advanced nanotechnology. In the last few years, InTech scientific publisher has been taking the initiative of helping worldwide scientists to share and improve the methods and the nanowire technology. This book is one of InTech's attempts to contribute to the promotion of this technology.

### **How to reference**

In order to correctly reference this scholarly work, feel free to copy and paste the following:

Feng Shi (2011). GaN Nanowires Fabricated by Magnetron Sputtering Deposition, Nanowires - Fundamental Research, Dr. Abbass Hashim (Ed.), ISBN: 978-953-307-327-9, InTech, Available from:  
<http://www.intechopen.com/books/nanowires-fundamental-research/gan-nanowires-fabricated-by-magnetron-sputtering-deposition>

**INTECH**  
open science | open minds

### **InTech Europe**

University Campus STeP Ri  
Slavka Krautzeka 83/A  
51000 Rijeka, Croatia  
Phone: +385 (51) 770 447  
Fax: +385 (51) 686 166  
[www.intechopen.com](http://www.intechopen.com)

### **InTech China**

Unit 405, Office Block, Hotel Equatorial Shanghai  
No.65, Yan An Road (West), Shanghai, 200040, China  
中国上海市延安西路65号上海国际贵都大饭店办公楼405单元  
Phone: +86-21-62489820  
Fax: +86-21-62489821

© 2011 The Author(s). Licensee IntechOpen. This chapter is distributed under the terms of the [Creative Commons Attribution-NonCommercial-ShareAlike-3.0 License](#), which permits use, distribution and reproduction for non-commercial purposes, provided the original is properly cited and derivative works building on this content are distributed under the same license.

IntechOpen

IntechOpen